



Permeability effects assessment on recovery performances of small-scale ORC plant

Fabio Fatigati^{*}, Davide Di Battista, Roberto Cipollone

University of L'Aquila, Department of Industrial and Information Engineering and Economics, Via Giovanni Gronchi, 18, L'Aquila, Italy

ARTICLE INFO

Keywords:

Waste Heat Recovery
Organic Rankine Cycle
ORC plant theoretical model
ORC hydraulic permeability
Volumetric pump and expander design optimization

ABSTRACT

Waste heat recovery (WHR) of internal combustion engine (ICE) exhaust gases through organic Rankine cycle (ORC)-based power units is one of the most effective technological alternatives to increase ICE efficiency, thereby limiting CO₂ emissions. Nevertheless, for an optimum design of components and plants, the assessment of intimate ORC-based plant behaviour is a key factor. This is the case of the mass-based permeability of the plant, which represents its attitude to be crossed by the working fluid, defining a specific relation between the mass flow rate and maximum achieved pressure level. Indeed, it was experimentally found that when the pump and expander are volumetric machines, a univocal relation exists between the operating parameters. Thus, the permeability relation defines certain operating paths of the ORC plant, limiting the domain in which the physical quantities can vary and ensuring the prediction of deviations from the ideal design behaviour. The concept of permeability has not been deeply addressed in the literature despite its importance; thus, it was deepened in this study through experimental and theoretical approaches. In particular, the knowledge acquired through a broad experimental campaign allowed us to obtain a physically based relationship, highlighting the main terms which influence this parameter. These terms are then grouped into dimensionless factors that orient the design and outline an easily implementable model-based control of the maximum plant pressure. Theoretical analyses were conducted through a comprehensive mathematical model of the recovery unit validated by an experimental campaign developed on a fully instrumented ORC test bench fed by the exhaust gases of a 3 L turbocharged diesel engine. The results indicate that the maximum values of the recovered power and efficiency are 3 kW and 4.4%, respectively.

1. Introduction

At present, the main driver in scientific and technical research in internal combustion engines (ICEs) is the development of new technologies that reduce greenhouse gas emissions, while maintaining their performance close to traditional driving expectations. The on-the-road transportation sector is responsible for almost 15% of CO₂ emissions into the atmosphere [1]. To limit this contribution, governments worldwide have provided strict limitations, introducing severe penalties if the limits are not adhered to. To meet these targets, several technologies have been developed to improve the efficiency of ICEs [2,3]. Among these solutions, waste heat recovery (WHR) from exhaust gases through ORC-based power units is certainly one of the most promising. Indeed, in exhaust gas, approximately 30–35% of the fuel chemical energy is lost.

Although ORC-based plants are well established in the market for

many industrial applications, several issues limit the full development of this technology in the on-the-road transportation sector. The main limitation is the size of the recovery unit, which does not exceed a few kilowatts [4]; this prevents expansion to wide technology, which exists for larger existing plants. Moreover, in mobile applications, the high-frequency variation of the hot thermal source (due to exhaust gas temperature and mass flow rate variations) makes it difficult to set up the design conditions of the components. Therefore, they frequently operate in under-designed or over-designed operating conditions, preventing the required functions (full vaporisation or condensation of the organic fluid, optimum expansion, insufficient pump pressure inlet, etc.) [5,6]. To limit the impact of these aspects, several control strategies have been developed; however, there is still room for improvement. There are also limiting aspects due to the interactions with the ICE and vehicles: backpressure produced by the heat recovery vapor generator (HRVG) is a problem that increases the specific fuel consumption of the ICE [7], additional vehicle's weight and space requirements on board reduce net

^{*} Corresponding author.

E-mail address: fabio.fatigati@univaq.it (F. Fatigati).

<https://doi.org/10.1016/j.applthermaleng.2021.117331>

Received 12 March 2021; Received in revised form 9 June 2021; Accepted 5 July 2021

Available online 10 July 2021

1359-4311/© 2021 Elsevier Ltd. All rights reserved.

Nomenclature*Symbols*

A	area [m ²]
dV	infinitesimal volume increase of the expander chamber [m ³]
F_N	normal force [N]
f	friction factor
h	specific enthalpy [J/kg]
\dot{m}	mass flow rate [kg/s]
P	power [W]
p	pressure [Pa], [bar]
$\dot{Q}_{t,rec}$	thermal power recovered [W]
\dot{q}	volumetric flow rate [m ³ /s]
N_v	number of expander vanes
r_v	distance between force application point and rotor centre [m]
R	specific gas constant (J/kgK)
T	temperature [K], [°C]
t	time [s]
V	volume [m ³]
V_{exp}	expander intake volume [m ³]
V_{pmp}	pump displaced volume [m ³]
Z	compressibility factor

Subscripts

amb	ambient conditions
base	baseline plant pressure
cond	condenser
cycle	expander cycle (one full rotation)
exh	exhaust
exp	expander
gas,in	temperature of gas entering the evaporator
gas,out	temperature of gas exiting the evaporator
glob	global
i	index of chamber
in	intake/inlet
ind	indicated

leak	leakages
loss	mechanical losses
mech	mechanical
Net,ORC	ORC net power
pmp	pump
rot	rotor
stat	stator
th	theoretical
vol	volumetric
w,in	cooling water temperature entering the condenser
w,out	cooling water temperature exiting the condenser
WF	working fluid

Greek Letters

α	permeability [kg/(sMPa)]
β_p	pressure ratio
β_{vol}	displacement ratio
$\beta_{\eta v}$	volumetric efficiency factor
β_ω	speed ratio
Δp	expander pressure drop [Pa], [bar]
ΔT_{SH}	superheating degree [K], [°C]
η	efficiency
ρ	density [kg/m ³]
ω	revolution speed [rpm], [rps]

Acronyms

BWR	backwork ratio
EG	electric generator
EM	electric motor
HRVG	heat recovery vapor generator
ICE	internal combustion engine
ORC	organic Rankine cycle
PHX	plate heat exchanger
SVRE	sliding vane rotary expander
TM	torque meter
WF	working fluid
WHR	waste heat recovery

recovered energy [8], and condensing situations related to the temperature of the external air which can be increased, thereby limiting the expansion and reducing recovery. The most critical component is the condenser and its integration [8,9]. Considered together, these aspects make the design and operation of the recovery unit a challenge not yet completely solved [10].

Therefore, the optimisation of the recovery unit in design and off-design conditions is fundamental for the success of this technology [11,12], and for clearing the way to a massive market introduction. For instance, multi-objective optimisation has been proposed to evaluate the effects of evaporation and condensation temperatures, superheating degree, and eventual mass fraction of zeotropic mixtures [13]. Suitable working fluids should have a boiling point as close as possible to the heat sink temperature, high critical pressure, and high molecular weight. R141b, R123, and R245fa have high thermodynamic performances [14]. For lower temperatures (such as in light-duty engines), more recent suitable fluids are CFO-1233zde, HFE-245fa2, HFO-1336mzz, HFE-347mcc, HFE-245cb2, and Novec 6, whereas for higher temperatures (heavy-duty engines), more suitable fluids include cyclopentane, ammonia, HCFO-1233zde, HFE-245fa2, and HFO-1366 m [15]. However, introducing concerns about safety and environmental impacts, R245fa and R245ca have been found to be the most suitable working fluids [16]. Furthermore, the working fluid charge and liquid receiver size can be optimised to maximise the overall plant performance

[17,18].

The transient nature of a recovery unit fed by the exhaust gases of an ICE is among the most complex aspects, the understanding of which allows setting the control strategy of the recovery unit [19]. In fact, once the main components (HRVG, expander, condenser, etc.) have been designed according to the specific operating conditions of the engine (gas flow rate and inlet temperature to the HRVG), when the engine working point changes, the components behave as they are under-designed or over-designed with respect to the new flow rate and temperature of the exhaust gas. For example, the flow rate entering the expander may not be able to be fully vaporised, or the superheating could be greater than the maximum allowable value for the working fluid to prevent thermal degradation. A flow rate significantly lower than the design rate can produce insufficient pressure at the expander inlet. An appropriate expander technology selection represents the key element to face transient requirements owing to variable engine operating conditions [20]. Volumetric expanders should be preferred to turbomachines, owing to their lower revolution speed and their capability to operate smoothly under unsteady conditions [21,22]. Rotating expanders represent a good choice for small-and micro-scale units [23]. Hence, the expander is retained as the key component of the whole unit, and its performance affects the working conditions of the entire plant. Volumetric losses in this machine affect not only the expander performance but also the thermodynamic cycle conditions [24]. In fact, it was

determined that the higher the volumetric losses, the larger the mass flow rate circulating inside the plant for a given maximum pressure [25]. This aspect is fundamentally important because volumetric losses represent the main limiting factor in volumetric machines, regardless of the volumetric technology, i.e. screws, [26,27] pistons [28,29], scrolls [30,31], or vane expanders [32–34].

The relation between the mass flow rate and the maximum pressure of the ORC-based unit is defined as ‘permeability’, which represents the attitude of the plant to be crossed by working fluid. This concept has been studied by the authors through experimental and numerical characterisation focused on sliding rotary vane [35] and scroll expanders [36], and a secondary injection port was introduced to improve this feature [37,38]. For both machine types, it was found that their permeability, expressed as the ratio of the mass flow rate to the pressure ratio, defines a univocal relation between these two quantities. In particular, if the working fluid enters the expander as superheated vapour, the intake pressure (i.e. ORC evaporating pressure) grows linearly with the mass flow rate. Nevertheless, all these developments focused on the expander behaviour, and the effects on the whole system were not assessed. In fact, the permeability represents an intrinsic plant property, which should be considered when the analysis is pushed towards a greater level of plant detail. Permeability fixes, for a given flow rate, the maximum operating pressure of the recovery unit, which influences the cycle efficiency, the behaviour of the expander, and, definitively, the power output of the unit. In addition, the power required by the pump is not negligible; therefore, its performance variation should be carefully considered. Moreover, as the permeability influences the evaporating pressure when volumetric machines are adopted, it affects the amount of thermal power recovered by the working fluid. Therefore, if this pressure is determined as the result of an optimisation of the cycle, under real conditions, it could deviate from the desired value.

All these effects on the overall performance of the recovery unit have not been fully and systematically considered in the literature. Thus, the introduction of the permeability concept can help to define the operating limits, allowing the integrated design of the machines to be carried out, and thus optimising the overall plant performance. Indeed, the definition of the permeability concept allows the implementation of a model-based control of the maximum plant pressure, which is of particular importance considering the wide working fluid flow rate variation due to the intrinsic enthalpy variation of the exhaust gas.

To fill this knowledge gap, in this work, the permeability conceptualisation was deepened, finding theoretical relations which correlate the permeability to the combination of pump and expander features. Owing to the knowledge acquired during an intense experimental campaign, several non-linearities characterising the permeability equations were solved, thereby achieving a linear dependence between the evaporating pressure (maximum pressure) and operating and design parameters of volumetric machines. In this novel mathematical representation, three dimensionless groups of parameters can be recognised:

- displaced volume of the pump and intake volume of the expander which provide information on the designed geometry of both volumetric machines;
- revolution speeds of the pump and expander that introduce actual operating quantities usually used to control the unit;
- volumetric efficiencies of the pump and expander which represent the deviation from the expected machine performance due to ageing, lubrication conditions, and other aspects that are not easily predictable.

The permeability representation based on dimensionless parameters provides a novel strategy for the integrated design of a volumetric pump and expander to maximise plant performance. Moreover, as the ORC control is mainly performed by acting on a combination of pump and

expander speed regulation, the developed analysis defines the speed ratio when the mass flow rate changes.

Finally, a mathematical model of the plant was developed to evaluate the influence of the dimensionless parameters introduced and the performance of the pump, expander, and entire plant under different upper thermal conditions. The model was validated through a wide experimental campaign conducted on an ORC-based power unit fed by the exhaust gases of a 3 L turbocharged diesel engine. Once validated, it was used as a software platform to perform ORC plant analysis, thereby defining design and operating optimisation strategies.

2. Experimental set-up

To characterise how plant permeability is affected by the main parameters of an ORC-based power unit, an experimental campaign was carried out on a test bench, where the upper thermal source is represented by the exhaust gases of a 3 L turbocharged diesel engine.

The experimental test bench is shown in Fig. 1(a), where the following main components can be recognised:

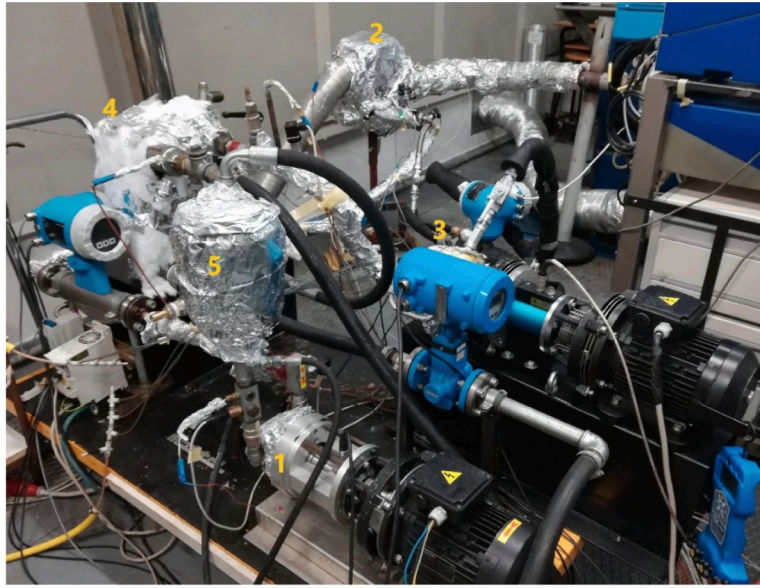
1. a gear pump, moved by an asynchronous electric motor and variable-revolution-speed actuation;
2. a tube and fin HRVG, where the working fluid receives thermal power from the upper thermal source;
3. a sliding vane rotary expander (SVRE) which is responsible for mechanical energy conversion; it drives a grid-connected electrical asynchronous generator whose speed is fixed at 1500 rpm;
4. a plate heat exchanger (PHX) at the expander exit, cooled by tap water;
5. a 3 L tank upstream of the pump to dump mass flow rate fluctuations and to guarantee a sufficient mass rate of the fluid to the pump (ensure a pressure level at the pump inlet which avoids cavitation).

R236fa was selected as the working fluid for the sake of continuity from previous experimental campaigns [35,36] and for its similar density to that of R245fa, which is one of the most suitable fluids for application under study. Indeed, although the properties of the two fluids (in terms of the intake temperature and exhaust pressure) are different at the design point (Table 1), the densities are comparable. Thus, the adoption in the two cases of the same expander (with an intake volume V_{exp} of 5.4 cm³ and a volumetric efficiency η_{vol} of 0.6) ensures a similar mass flow rate when the intake pressure is the same. This means that the design of the expander (which is the most crucial component) is quite similar considering the two fluids. Indeed, a machine designed to work with R236fa can also operate with R245fa by adapting the volume ratio (by dividing the exhaust volume by the intake volume) as the pressure ratio β_p (equal to the intake-to-exhaust pressure ratio) in the two cases is different. Moreover, R245fa corresponds to a higher evaporation temperature when the pressure is 12 bar, slightly modifying the thermal exchange with the upper thermal source.

To lubricate the volumetric machines, an ISO VG 68 POE oil is mixed into the working fluid in a quantity of 5% of the whole R236fa mass charged in the plant, which is equal to 6 kg.

The ORC-based plant is fully instrumented, as shown in Fig. 1(b). The pressure and temperature are measured upstream and downstream of each component to reconstruct the thermodynamic cycle of the organic fluid. The mass flow rate is directly measured using a Coriolis flow meter, and an additional magnetic flow meter measures the flow rate of the cooling water at the condenser. The torque and revolution speed of the expander and pump are measured using dedicated torque meters. Moreover, with the introduction of a set of piezoresistive sensors inside the expander casing, the pressure inside the vane during rotation can be reconstructed to directly evaluate the indicated power.

The steps of the experimental tests are summarized as follows:



(a): Experimental test bench. 1 - pump; 2 - HRVG; 3 - SVRE; 4 - PHX condenser; 5 – tank.

Fig. 1a. Experimental test bench. 1 - pump; 2 - HRVG; 3 - SVRE; 4 - PHX condenser; 5 – tank.

Table 1

R236fa and R245fa properties corresponding to design conditions.

	R236fa	R245fa
Expander intake pressure p_{in} [bar]	12	12
Expander intake temperature T_{in} (evaporation temperature at p_{in}) [°C]	88.3	107.7
Expander intake density ρ_{in} [kg/m ³]	79.0	70.4
Expander revolution speed ω_{exp} [rpm]	1500	1500
Mass flow rate working fluid \dot{m}_{WF} [kg/s]	0.124	0.111
Expander exhaust pressure p_{exh} (evaporation pressure at $T_{exh} = 40$ °C) [bar]	4.4	2.5
Pressure ratio β_p	2.7	4.8

- 1 A specific operating point of the ICE is set in terms of torque and revolution speed, thus defining the thermal power of the exhaust gases entering the evaporator (HRVG).
- 2 Based on the high thermal source condition (exhaust gases), the pump speed is chosen to provide a certain flow rate to ensure that the working fluid enters the expander, at least as vapour.
- 3 When the steady-state condition is reached by the ORC plant, the data are registered using a proprietary script for a time of 5 s. The acquisition frequencies are set to 4500 Hz to ensure that the piezoresistive sensors can capture the pressure inside the chambers every 2° of expander shaft rotation.
- 4 After the acquisition, the raw data are postprocessed.
- 5 The same working point has been repeated at least three times to smooth possible measurement deviations.

The measurement uncertainty is reported for each device in Table 2.

3. Permeability analysis

Hydraulic permeability is preliminarily defined as the attitude of the plant to be crossed by the working fluid [35]. It was found that the permeability is mainly determined by the expander performance. Indeed, the higher the expander permeability, the lower the pressure levels observed within the plant. Therefore, the permeability can be analytically defined as the ratio of the mass flow rate entering the expander to the pressure difference between the expander intake and

exhaust sides Δp_{exp} (1):

$$\alpha_{ORC} = \frac{\dot{m}_{WF}}{\Delta p_{exp}} \quad (1)$$

Hence, a hydraulic model of the plant was developed, which represents the entire ORC-based power unit by volumetric machines, as shown in Fig. 2.

The pump defines the mass flow rate circulating inside the plant according to Eq. (2):

$$\dot{m}_{WF} = \rho_{pmp,in} V_{pmp} \eta_{vol,pmp} \omega_{pmp} \quad (2)$$

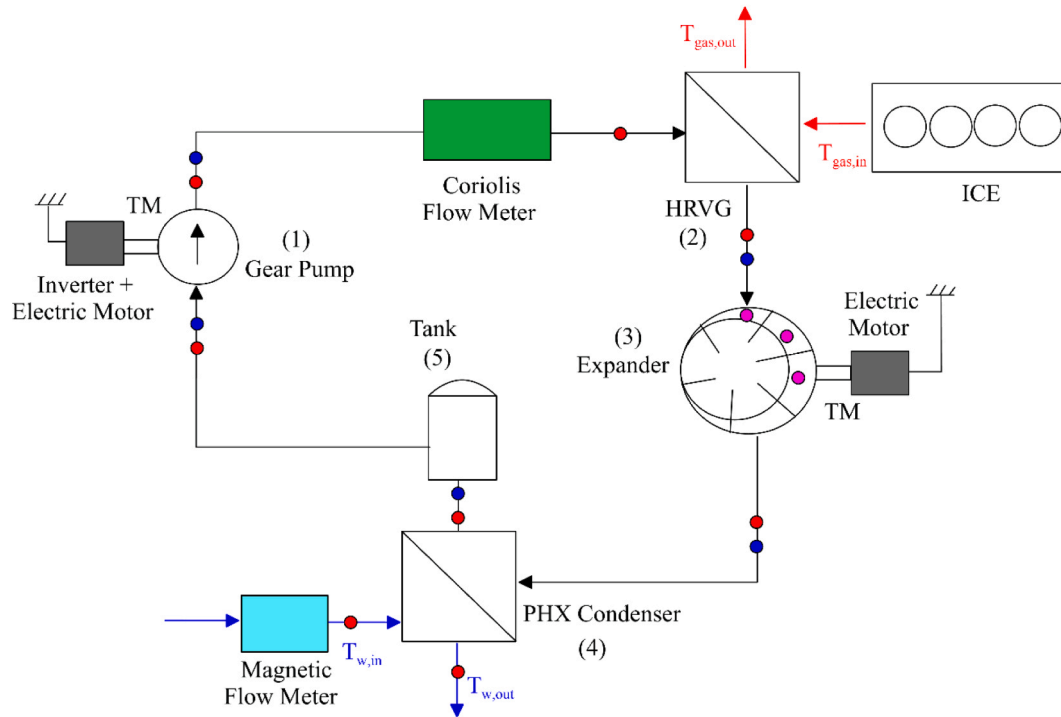
Thus, the parameter which defines the mass flow rate circulating through the plant is the pump revolution speed. Indeed, the displacement of the pump (V_{pmp}) is given, and the volumetric efficiency $\eta_{vol,pmp}$ is a property of the pump, though it depends on the aging, pressure delivered, etc. Again, the density of the working fluid ($\rho_{pmp,in}$) strictly depends on temperature and pressure; because it is in the liquid phase at the pump intake, this parameter does not exhibit significant variations.

In an ORC-based plant, the pipes, evaporator, and condenser can be considered as a source of distributed and concentrated pressure drops. As these components are properly designed, the pressure drop is negligible with respect to that observed across the expander or pump [35]. Fig. 3 shows the measured pressure in different plant sections, indicating that most of the pressure delivered by the pump Δp_{pmp} is due to the expander, which is therefore the main contributor to the two pressure levels within the plant. Fig. 3 also shows the base pressure of the plant p_{base} when the charged mass of R236fa is 6 kg and no thermal exchanges with the high and low thermal sources take place. The pressure corresponds to a steady condition in which the pump does not deliver the mass flow rate, and the plant reaches thermal equilibrium with the surrounding environment.

As can be observed from the experimental measures reported in Fig. 4(a), p_{base} is sensitive to the charge of the working fluid only in the first steps of the charging process, when its amount is negligible compared to the volume of the whole plant (11 L). When the mass reaches the definitive value (6 kg), the base pressure p_{base} is essentially constant, and it is close to the saturation pressure of the fluid at the ambient temperature, which in the considered experimental case is equal to 13 °C. This means that the working fluid inside the plant when it

Legend

- Termocouples
- Pressure transducers
- Piezo-resistive pressure transducers
- TM Torque Meter
- PHX Plate Heat Exchanger
- HRVG Heat Recovery Vapor Generator



(b): Schematic of the experimental test bench and the measurement instruments.

Fig. 1b. Schematic of the experimental test bench and the measurement instruments.

Table 2
Uncertainty of the measurement instruments.

	Sensor type	Operating range	Uncertainty
Working fluid temperature	RS™ T-type thermocouple	-75 to 220 °C	±1 °C
Working fluid pressure	Wika™ membrane pressure sensor	0–16 bar	±0.3 bar
Indicated cycle (pressure inside the expander chambers)	Kistler™ piezoresistive sensor	0–10/20 bar	±0.1% of full-scale sensor output
Working fluid mass flow rate	Endress Hauser™ Promass 80 Coriolis mass flow meter	0–2000 kg/h	±0.15% (kg/s)
Water mass flow rate	Krohne™ IFC 80 electromagnetic flow-meter	0–5.4 m³/h	±0.3% (kg/s)
Expander torque	Kistler™ 4503 A	0–10/50 Nm	0.02 Nm
Expander speed		0–12000 rpm	1 rpm
Pump torque	Kistler™ 4502 A	0–10 Nm	0.02 Nm
Pump speed		0–12000 rpm	1 rpm

does not exchange thermal power with the high and low thermal sources in a two-phase condition.

When the plant starts to exchange thermal power with the high and low thermal sources, the minimum plant pressure (at pump intake) is larger than the base pressure. Moreover, the minimum pressure increases with the mass flow rate, which is enhanced to follow the thermal

power availability at a high thermal source (Fig. 4(b)). This is due to the linear growth of the coolant average temperature at the condenser with mass flow rate, and hence, the available thermal power.

Therefore, the plant maximum pressure is defined by the expander, which has the role of converting thermodynamic energy into mechanical energy, and expanding the mass flow rate delivered by the pump. Indeed, the flow across a volumetric machine is not continuous (through-flow), but it is forced into periodic phases. Hence, the machine performs an intake, an expansion, and an exhaust phase, thereby breaking the continuity of the flux. Nevertheless, as the machine rotation rate is relatively high (1500 rpm in the experimental facility, fixed by the connection of the asynchronous generator to the electric grid), the machine performs several cycles per second (25 Hz); thus, mass pulsation is not evident and the flow appears as continuous. Therefore, this feature of the device defines the pressure regimes of the plant according to the circulating mass flow rate. The mass flow rate processed by the expander can be expressed as follows:

$$\dot{m}_{WF} = \frac{\rho_{exp,in} V_{exp} \omega_{exp}}{\eta_{vol,exp}} \quad (3)$$

Eq. (3) is the base of plant permeability represented by the equilibrium of mass provided by the pump and that processed by the expander. It is important to note that the minimum plant pressure affects the permeability; indeed, this parameter, together with the plant maximum pressure, defines the pressure difference at the expander intake/exhaust side. This quantity represents the main driver of volumetric losses [25] which lead to an increase in permeability. Owing to the volumetric efficiency, this indirect effect can be considered.

To date, the permeability was expressed only by referring to the expander behaviour (right term of (3)) [35] neglecting the role of the

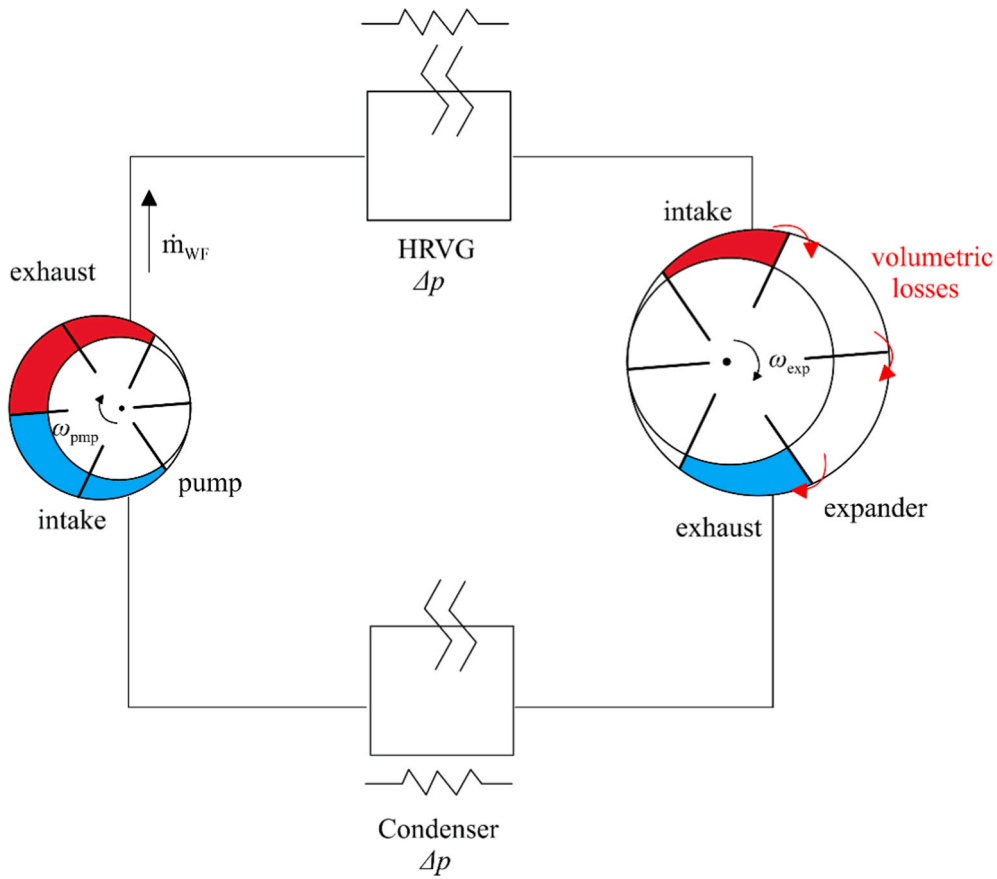


Fig. 2. Sketch of hydraulic model of ORC-based power unit. Pump and expander are represented by equivalent sliding rotary vanes.

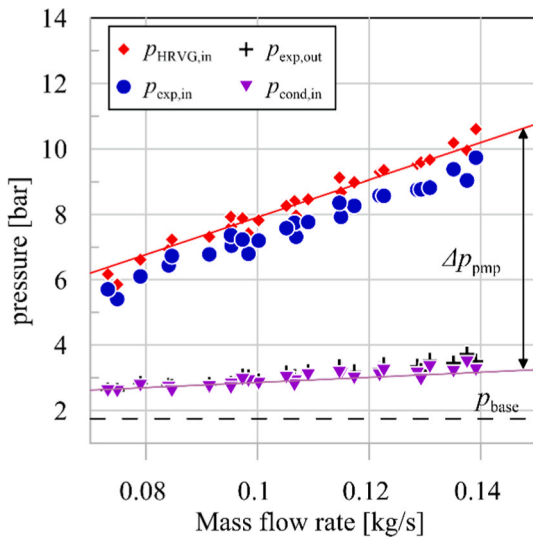


Fig. 3. Pressure values upstream and downstream of each ORC component. P_{base} refers to the base pressure defined by the quantity of the fluid inside the plant and its temperature.

pump. The pump behaviour affects the elaborated mass flow rate (left term of (3)), which can be expressed as a function of the density of the working fluid at the pump intake, pump displacement volume, volumetric efficiency, and revolution speed. Thus, the mass conservation Eq. (3) can be expressed as in (4) as a function of the operating and design parameters of the pump and expander.

$$\rho_{pmp,in} V_{pmp} \eta_{vol,pmp} \omega_{pmp} = \frac{\rho_{exp,in} V_{exp} \omega_{exp}}{\eta_{vol,exp}} \quad (4)$$

In (4), the left term represents the mass flow rate delivered by the pump, whereas the right term is related to the hydraulic impedance of the expander and, thus, of the circuit. This impedance is defined as the mass flow rate elaborated by the expander. Thus, for a given expander revolution speed, in the right term, the only parameter that can be varied during the operation is the working fluid density. The expander intake volume V_{exp} is a design parameter, whereas the expander volumetric efficiency is defined by the constructive gap and unpredictable quantities. Thus, for each mass flow rate sent by the pump, the working fluid density varies according to mass conservation. The density of the working fluid, however, also depends on the temperature and pressure of the working fluid at the intake of the expander. Therefore, to assess the thermodynamic relation, similar to what was done in [35], the ideal gas law (5) (corrected by a compressibility factor to consider the real behaviour of the working fluid) was considered in the analysis, according to (5).

$$\frac{P_{exp,in}}{\rho_{exp,in}} = ZRT_{exp,in} \quad (5)$$

By substituting (5) in (4), a novel expression for permeability can be obtained as follows:

$$P_{exp,in} = \frac{ZRT_{exp,in} \eta_{vol,exp}}{V_{exp} \omega_{exp}} \rho_{pmp,in} V_{pmp} \eta_{vol,pmp} \omega_{pmp} \quad (6)$$

Eq. (6) represents the intake pressure at the expander as a function of the expander, pump design, and operating parameters. Therefore, this relation provides additional value to the permeability concept with respect to the previous relation [35], which considers only expander

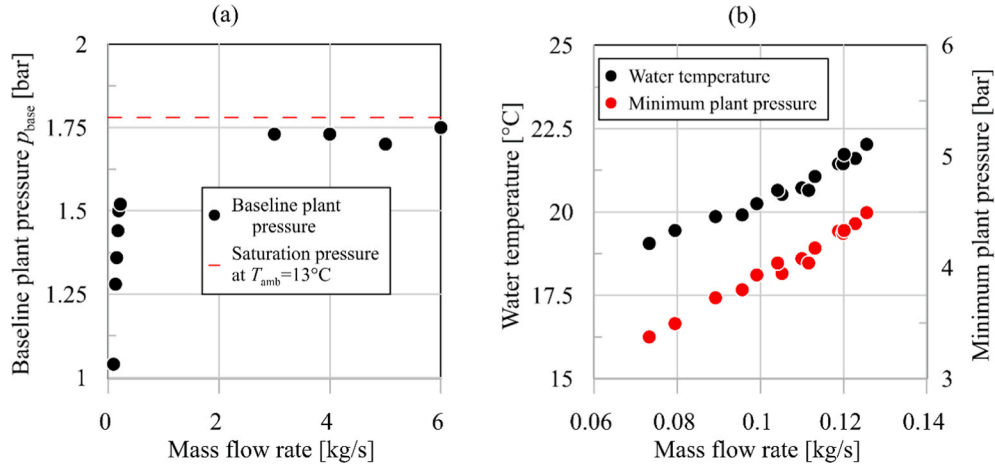


Fig. 4. Effect of charge of working fluid on baseline pressure (a); Water temperature at the condenser and minimum plant pressure vs mass flow rate (b).

features (7):

$$p_{exp,in} = \frac{ZRT_{exp,in}\eta_{vol,exp}}{V_{exp}\omega_{exp}} \dot{m}_{WF} \quad (7)$$

Rearranging the terms of the novel form of mass conservation expressed in (6), the pump and design parameters can be grouped per type. Thus, the permeability can be expressed as a function of the dimensionless operating parameters of the pump and expanders (8):

$$p_{exp,in} = ZRT_{exp,in}\rho_{pmp,in}\beta_{vol}\beta_{\omega}\beta_{\eta_V} \quad (8)$$

where:

$$\beta_{vol} = \frac{V_{pmp}}{V_{exp}} \quad (8.1)$$

$$\beta_{\omega} = \frac{\omega_{pmp}}{\omega_{exp}} \quad (8.2)$$

$$\beta_{\eta_V} = \eta_{vol,pmp}\eta_{vol,exp} \quad (8.3)$$

Thus, β_{vol} (8.1) represents the dimensionless ratio of the pump displacement to expander intake volume. This parameter relates the design choice of machines with plant permeability. The higher this ratio, the larger is the plant maximum pressure achieved for a given mass flow rate. The numerator is directly proportional to the mass flow rate delivered by the pump, whereas the denominator is proportional to the mass flow rate elaborated by the expander. In other words, given a constant pump volume, the lower the expander intake volume, the higher is the plant hydraulic impedance.

β_{ω} (8.2) represents the dimensionless ratio of the expander to pump revolution speeds. The maximum pressure increases, enhancing this parameter. Indeed, the numerator (pump speed) is proportional to the mass flow rate circulating inside the plant, whereas the denominator (expander speed) is related to the expander hydraulic impedance. If the expander speed decreases (β_{ω} grows), the permeability decreases, enhancing the hydraulic impedance of the circuit. The pump revolution speed depends on the desired mass flow rate of the pump. For each pump geometry, there is only one revolution speed that ensures the desired mass flow rate (if the volumetric efficiency does not vary significantly).

β_{η_V} (8.3) depends on the product of the volumetric efficiencies of the two devices. Therefore, it increases when both volumetric efficiencies grow. Indeed, if the pump volumetric efficiency increases, for a certain pump revolution speed and displaced volume, a higher mass flow rate can be sent and enter the expander. Again, if the volumetric efficiency of the expander increases, the mass flow rate sent by the pump which enters the machine increases, without escaping across clearances, leading to a higher ORC maximum pressure.

Therefore, (8) enables a novel integrated approach to considering plant permeability, not only related to the expander but also to the whole plant as a function of the operating conditions of the pump and the expander. Moreover, considering all the design factors reported in (8), it is clear that the permeability depends on the definition of each β ratio. In this way, it is possible to define the impact of each quantity on plant performance (permeability) and, for a given mass flow rate of the fluid principally fixed by the degree of heat recovery at the HRVG, the maximum pressure of the plant, i.e. the saturation condition.

3.1. Permeability experimental characterization

In the previous section, permeability was represented as a linear relation between the intake pressure and mass flow rate. Nevertheless, from a more detailed analysis, it is evident that the non-linearity between the expander intake pressure and temperature of the working fluid can be captured as the non-linear variation of the vaporisation temperature with respect to pressure. Therefore, (8) can be further expressed as in (9).

$$p_{exp,in} = ZR(T_{exp,in}(p_{exp,in}) + \Delta T_{SH})\rho_{pmp,in}\beta_{vol}\beta_{\omega}\beta_{\eta_V} \quad (9)$$

where (9) also shows the role of the superheating degree ΔT_{SH} , which is a design parameter; however, during operation of the unit, it changes according to many parameters. Nevertheless, in a real application, the impact of this parameter is low, as ΔT_{SH} is generally lower than 20 $^\circ\text{C}$ [35]. This is evidenced in Fig. 5(a), where the experimental results in terms of the intake pressure variation as a function of mass flow rate and intake temperature are reported. It can be observed that the deviations from linearity are limited. Indeed, as Fig. 5(b) shows, when the superheating degree increases from 6 to 20 $^\circ\text{C}$, the intake pressure linearly grows from 9.2 to 10.2 bar, keeping the mass flow rate of the working fluid constant at 0.1 kg/s. This means that a maximum pressure excursion of 1 bar (on an average intake pressure of 9.7 bar) can be retained. The excursion is even lower, considering that the compressibility factor varies between 0.8 and 0.82 for the same interval of superheating degree, as evaluated from the real properties of the fluid. Moreover, the density of the working fluid at the pump intake is constant, as it is always in the subcooled condition at this operating point. Thus, the intake pressure changes linearly with respect to the three β parameters.

As previously discussed, the increase in the three β -parameters ensures the growth of the expander intake pressure and, consequently, the plant maximum pressure. With respect to β_{vol} , once the design of the pump and expander has been developed, this parameter can no longer be changed. For the experimental case, β_{vol} is nearly equal to 2, as the pump displacement and expander intake volume are respectively equal to 11.2 and 5.4 cm^3 . Therefore, to increase the maximum plant pressure,

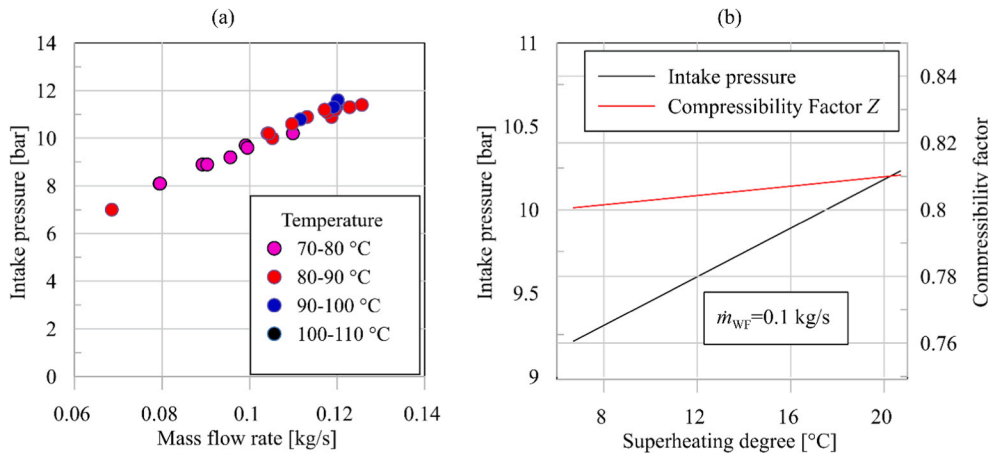


Fig. 5. Experimental trend of intake pressure as a function of mass flow rate, taking the corresponding temperature as a parameter (a); Experimental fitting of intake pressure and compressibility factor trend as a function of superheating degree (b).

β_{vol} should be enhanced, and this can be achieved by increasing the pump displacement or reducing the expander intake volume.

In contrast to β_{vol} , the speed ratio β_{ω} is an operating parameter, such that it can be varied for regulation purposes by varying the pump speed (numerator) or expander speed (denominator). Indeed, the expander speed can be regulated by acting on the load resistance, whereas state-cycle parameters such as expander inlet pressure and temperature can be varied by acting on pump parameters according to the approach described in [39].

If β_{ω} is varied by acting on the pump speed and keeping the expander constant, the regulation purpose regards the mass flow rate circulating inside the plant, which must match the thermal power available at a high thermal source to be recovered. Thus, in this case, the intake pressure increases because β_{ω} is associated with an increase in the mass flow rate. On the contrary, if the mass flow rate must be set equal to the design value, there is only a pump speed, which ensures that the requirement is fulfilled once V_{pmp} and hence β_{vol} are defined. In this case, there are only a limited number of V_{pmp} and ω_{pmp} values which allow elaborating the required mass flow rate; thus, the only way to vary β_{ω} is to act on the expander speed. In other words, the expander speed is a free parameter that can be varied to increase or decrease the plant permeability for a fixed mass flow rate of the fluid.

Thus, the following conclusions can be drawn with respect to β_{ω} :

- β_{ω} can be varied by varying the pump speed while keeping the expander speed constant if the mass flow rate should be adjusted depending on the thermal power available at a high thermal source. In this case, the plant permeability remains constant as the expander conditions do not change.
- For a given mass flow rate, once the pump displaced volume is chosen, the pump speed is univocally defined, and β_{ω} varies with the expander speed. In this case, an increase in β_{ω} (expander speed diminishes) leads to a decrease in permeability, whereas a β_{ω} reduction (increase in expander speed) ensures a permeability gain. Moreover, for the same mass flow rate range (and consequently pump speed interval), if the expander speed increases, the speed ratio range (and values) diminishes, leading to a higher permeability. On the contrary, if a lower expander speed is selected for the same mass flow rate range, the speed ratio interval assumes higher values and a wider range.

In the experimental case, $\beta_{vol} = 2$ and the expander revolution speed was maintained at 1500 rpm as it was connected to the electric network; thus, β_{ω} changed only because the pump speed varied to elaborate the required mass flow rate (Fig. 6). Therefore, for the mass flow rate range considered (0.07–0.14) kg/s, the pump speed varies between 300 and

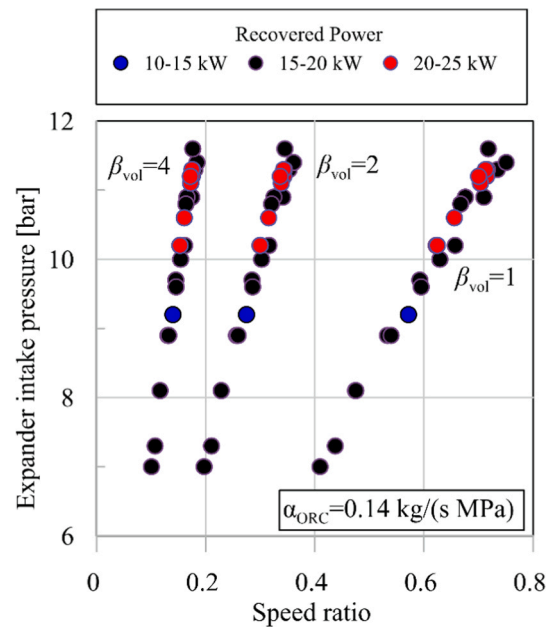


Fig. 6. Effects of speed ratio β_{ω} on plant permeability keeping constant expander speed ($\omega_{exp} = 1500 \text{ rpm}$), with volume ratio β_{vol} taken as a parameter.

600 rpm; thus, although the speed ratio ranges from 0.2 to 0.4, no effects on permeability (equal to 0.14 kg/(s MPa)) are observed because the expander conditions are kept constant.

The permeability does not change when choosing a different pump size, nor when consequently adopting another β_{vol} . Indeed, to fulfil the same mass flow rate range, the pump speed must vary in an appropriate interval (Fig. 6). Therefore, for a certain expander speed and displaced volume, if a lower V_{pmp} is chosen (5.4 cm³), a β_{vol} equal to 1 is obtained and the pump must rotate at a higher speed (850–1051 rpm) to elaborate the required mass flow rate. Thus, although in this case the speed ratio β_{ω} increases (0.4–0.8) the intake pressure interval and mass flow rate do not change, such that the permeability is equal to 0.14 kg/(s MPa) as in the experimental case ($\beta_{vol} = 2$).

The permeability value is also predicted when a higher V_{pmp} is selected ($V_{pmp} = 22 \text{ cm}^3$), resulting in a larger β_{vol} value of 4. The difference, in this case, is that the curve is shifted leftward in Fig. 6 as the pump must rotate at a slower speed (210–257 rpm) to fulfil the same mass flow rate range. This means that considering a certain mass flow rate interval, V_{pmp} and ω_{pmp} are intrinsically constrained; nevertheless,

their variation does not affect the machine permeability, but rather only the pump performance. This means that for a given mass flow rate interval, once V_{pmp} and ω_{pmp} are set to optimise the pump performance, the variations in V_{exp} and ω_{exp} allow the proper determination of plant permeability. Therefore, from a permeability perspective, β_{vol} and β_{ω} are determined by the expander parameters. However, although the pump design does not affect plant permeability, it affects the pump working conditions, as reported in Section 4.

The last dimensionless parameter is the volumetric efficiency factor $\beta_{\eta v}$, which is given by the product of the pump and the expander volumetric efficiencies. In a previous study [35], it was demonstrated that the expander volumetric efficiency highly impacts machine permeability. Indeed, if the expander volumetric efficiency is low, the expander should process a greater mass flow rate to achieve the same intake pressure, owing to volumetric losses [25]. The novel dimensionless approach allows the expression of the combined effect of the pump and expander volumetric efficiencies. In the experimental points of Fig. 7, the pump and expander volumetric efficiencies are equal to 0.9, and 0.6, respectively, leading to a $\beta_{\eta v}$ of 0.5, with a permeability (2) of 0.14 kg/(s MPa).

To show the effect of $\beta_{\eta v}$, a second set of experimental data was considered. This is associated with the same expander geometry and revolution speed, but with a lower volumetric efficiency (0.35). As the pump still has a volumetric efficiency of 0.9, $\beta_{\eta v}$ in this second case is equal to 0.3. In Fig. 7, the intake pressure is reported as a function of the β parameters for the two experimental cases. $\beta_{vol} = 2$ is considered for both cases, as the pump and expander have the same geometry. Considering β_{ω} , in the case of $\beta_{\eta v} = 0.5$, it varies between 0.2 and 0.35, whereas in the case of low $\beta_{\eta v}$ (0.3), β_{ω} is in the range of 0.25–0.5. This is because, in the case of an expander with a lower volumetric efficiency (0.35), a higher mass flow rate should be delivered by the pump to achieve the same intake pressure value of a low-permeability device (high volumetric efficiency). This can be noticed by observing that the maximum intake pressure (12 bar) is achieved with the speed ratio (proportional to mass flow rate) of 0.35 in the $\beta_{\eta v} = 0.5$ case, whereas the same pressure is obtained with β_{ω} higher than 0.5 when $\beta_{\eta v} = 0.3$.

Fig. 7 indicates that when $\beta_{\eta v}$ diminishes (e.g. for an insufficient lubrication condition or the aging of the device), the plant permeability increases owing to higher leakages. Indeed, when $\beta_{\eta v}$ is equal to 0.5, a plant permeability of 0.14 kg/(s MPa) is achieved, whereas for a lower $\beta_{\eta v}$ (0.3) the plant permeability is equal to 0.2 kg/(s MPa).

This is evidenced by the lower slope of the intake pressure with respect to the speed ratio (mass flow rate) when $\beta_{\eta v}$ decreases from 0.5 to 0.3 (Fig. 7). The permeability variations also affect the whole plant

behaviour. Indeed, if the permeability increases, a high mass flow rate should be delivered by the pump to achieve the same evaporating pressure (higher speed ratio) and to recover a higher thermal power from the exhaust gases. Indeed, if the target intake pressure is equal to 12 bar, the low-permeability plant ($\beta_{\eta v} = 0.5$) requires a recovered power in the range of 15–20 kW, whereas that of a high-permeability device ($\beta_{\eta v} = 0.3$) varies in the range of 30–35 kW.

In Fig. 7, considering an intake pressure of 10 bar, the less permeable expander ($\eta_{vol} = 0.5$) requires a mass flow rate of 0.1 kg/s (from the pump) to achieve this value with thermal power in the range of 10–15 kW. However, the pump must provide a mass flow rate of 0.14 kg/s if a higher permeable expander ($\eta_{vol} = 0.35$) is adopted with thermal power in the range of 25–30 kW.

3.2. Permeability model of the ORC-based power unit

The theoretical analysis above shows a novel integrated approach for representing the permeability as a function of the dimensionless parameters. Through the experimental analysis, it was observed that these parameters represent the mutual interaction between the pump and expander and plant permeability. Nevertheless, the experimental cases present several constraints, such as the fixed expander speed and the pump and expander displaced volumes. Thus, a mathematical model of the plant was developed and experimentally validated to advance the analysis. The main novelty introduced by the model is the representation of the plant feature through the permeability reproduction assessing not only the hydraulic effects, but also the effects in terms of the whole plant performance. This concept represents an important advancement with respect to the previous works of the authors regarding permeability. Indeed, in [35] the permeability was seen only from the expander perspective without exploiting and quantifying the effects on the whole plant performance. This was achieved by extending the permeability equations from the expander to the whole plant, thereby reproducing the interaction between the volumetric machines, which strongly affects the plant behaviour. A further new aspect introduced by the model is that it performs a plant analysis with a relatively simple mathematical structure; in general, ORC plant analyses are developed in dedicated numerical software platforms, which require longer computation time. This model simplification is obtained by solving certain non-linearities between the operating quantities, thanks to the wide experimental activity supporting the theoretical study. In this way, a relatively simple procedure was developed to reproduce real plant features. A further original aspect is that the model can be used to outline the effects of design and operating choice made on this machine on the permeability and the whole plant performance, thus representing a tool to properly conceive and define such components.

The theoretical model is divided into fluid and mechanical sections according to the scheme shown in Fig. 8. The fluid model was carried out considering the hydraulic scheme shown in Fig. 2. Based on the reported experimental data and theoretical analysis, some hypotheses were adopted to simplify the calculation and ensure that the entire behaviour of the ORC plant is represented in detail. As the pump and expander are volumetric, ideally, the entire circuit can be divided into two parts: the high-pressure circuit from the pump exhaust to the expander intake and the low-pressure circuit from the expander exhaust and pump intake. The expander divides the plant into two parts, behaving as a rotating valve. Thus, from a theoretical point of view, the minimum pressure does not affect the plant maximum pressure or, consequently, the permeability. Nevertheless, the two circuits are connected by the volumetric losses of the pump and expander; thus, the effect of the circuit operating at a low pressure should be considered. This effect passes through the volumetric efficiency (leakage across the expander), which can be expressed as a function of the pressure difference across the machine (input and exhaust expander pressure difference).

The theoretical base of the model is the permeability relation reported in (6). The modelling process consists of the following steps:

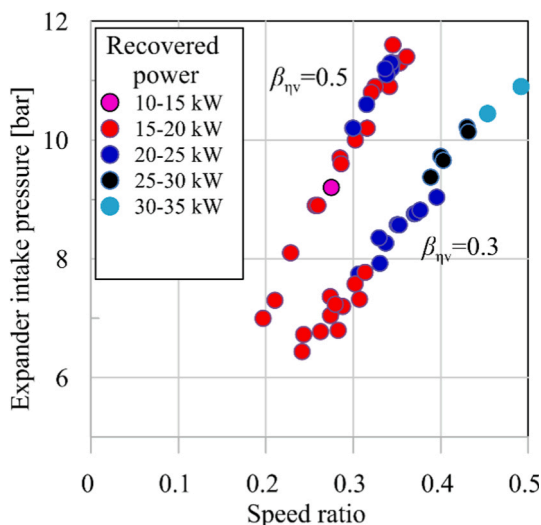


Fig. 7. Experimental assessment of the effects of $\beta_{\eta v}$ on plant permeability.

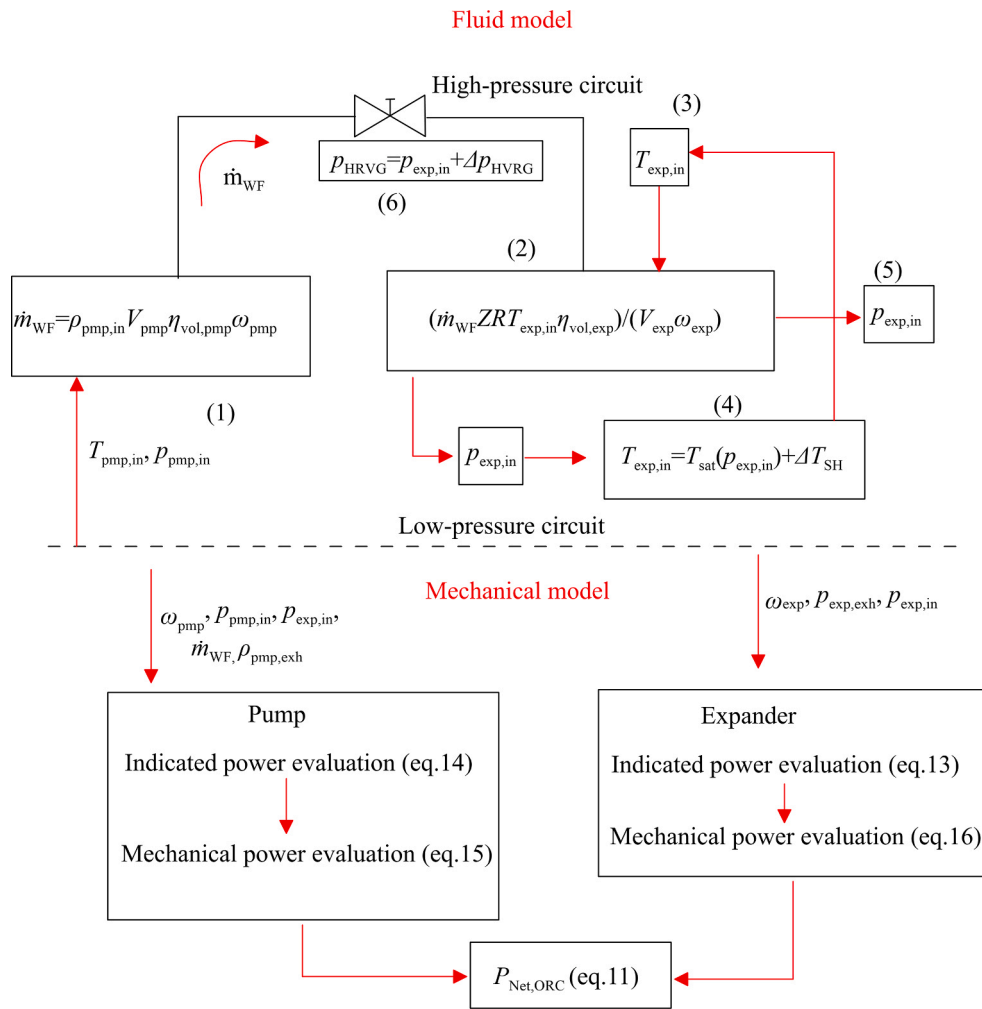


Fig. 8. Theoretical permeability-based model of the ORC-based power unit.

1. The mass flow rate provided by the pump is evaluated by determining the pump geometry (swept volume and volumetric efficiency) and operating conditions (revolution speed). Moreover, the density of the working fluid is introduced in the evaluation by knowing the inlet condition of the fluid.
2. The pressure at the expander intake is calculated according to mass conservation Eqn. (7). It is observed that the application of the conservation of mass returns the density in a closed form. However, to evaluate the pressure, the temperature of the working fluid must be known and introduced into the procedure. Its introduction produces a nonlinearity in model Eqn. (9); however, the experimental activity shows that for the adopted superheating degree range (10–20 °C), the influence of the working fluid temperature on the intake pressure is limited. Thus, the following simple iterative procedure is adopted:
3. An initial intake value of temperature should be introduced in the calculation to evaluate the expander inlet pressure (step 2).
4. The intake pressure value is introduced in step 4, and this allows the evaluation of the new value of the intake temperature considering the rated superheating degree of the working fluid (10–15 °C).
5. This updated intake temperature value is introduced in the permeability equation Eqn. (7) to obtain an updated intake pressure value, which is compared with that set in a), and the calculation ends when a small difference is reached; otherwise, the procedure is repeated until convergence is achieved. Generally, few iterations are sufficient to ensure a good accuracy, as temperature has a negligible effect on

the expander intake pressure definition if the fluid is at least fully vaporised and the superheating degree range is narrow.

6. The expander intake pressure coincides with the evaporating pressure (net pressure drop between the two machines). Therefore, once this parameter and the working fluid temperature are known, the thermal power recovered by the working fluid in this condition is evaluated through (10), which expresses the energy conservation at the HRVG (10):

$$\dot{Q}_{t,rec} = \dot{m}_{wf} (h_{HRVG,out} - h_{HRVG,in}) \quad (10)$$

To determine the relationship between permeability and ORC-based power unit performance, it is important to assess its effects on the net mechanical power produced by the unit. For this reason, the fluid model (upper section of Fig. 9) was integrated with the mechanical model of the pump and expander. The net power produced by the plant ($P_{Net,ORC}$) is equal to the difference between the expander and pump powers (11).

$$P_{Net,ORC} = P_{mech,exp} - P_{mech,pmp} \quad (11)$$

Fig. 8 shows the mechanical model structure and its connection with the permeability model. This model is subdivided into two parts:

- a). the pump section, which ensures the evaluation of the amount of mechanical power required to circulate the mass flow rate of the working fluid;
- b). the expander section, which evaluates the mechanical power produced by the expander.

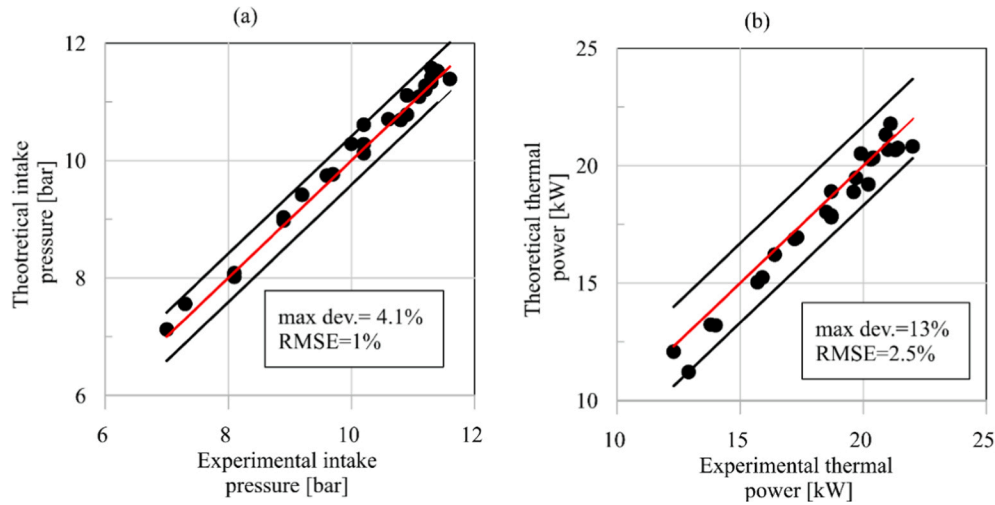


Fig. 9. Validation results: Comparison between experimental and predicted data of intake pressure (a) and thermal power recovered (b).

The permeability model provides the pump flow rate and the corresponding pressure rise.

Thus, the hydraulic power requested by the pump can be evaluated according to (12).

$$P_{\text{hyd}} = \dot{q}_{\text{WF}}(p_{\text{pmp,out}} - p_{\text{pmp,in}}) = \dot{q}_{\text{WF}}(p_{\text{exp,in}} + \Delta p_{\text{HRVG}} - p_{\text{pmp,in}}) \quad (12)$$

Eq. (12) applies to the ideal conditions. The work exchanged between the machine and the working fluid is due to the area of the indicated diagram, which represents the pressure values as a function of the machine volume (13).

$$P_{\text{ind}} = \frac{\sum_{i=1}^{N_v} \oint p_i dV_i}{t_{\text{cycle}}} \quad (13)$$

For volumetric pumps, the hydraulic power coincides with the indicated power only under ideal conditions, when the intake and exhaust phases are isobaric transformations and there are no volumetric losses which cause the delivered flow rate to be lower than the theoretical one. Generally, a volumetric pump does not perform closed-volume transformations, thus performing only the intake and exhaust phases. For this reason, to evaluate the indicated power, a simpler relation (14) with respect to (13) is considered. Eq. (14) allows the consideration of the leaked flow rate ($\dot{q}_{\text{WF,leak}}$) inside the pump, which leads not only to a volumetric loss but also to an energetic penalty, considering that this part of the working fluid is compressed but not sent. In (14), excursions from isobaric intake and exhaust processes are not considered, as this would require the development of a fluid-dynamic model of the transient phenomena occurring in the intake/exhaust adduction pipe. The reproduction of such phenomena would certainly ensure a more detailed representation of the real pump behaviour; however, as the aim of the model is to determine the relationship between permeability and the whole plant performance, the indicated power can be simplified. In a more detailed treatment reported in [40] the authors provide a deeper contribution. Moreover, if the pump ports are properly designed, the pressure loss during the intake and overpressure during the exhaust can be limited. Thus, (14) represents a reasonable compromise between the accuracy and simplicity of the model.

$$P_{\text{ind}} = (\dot{q}_{\text{WF}} + \dot{q}_{\text{WF,leak}})(p_{\text{pmp,out}} - p_{\text{pmp,in}}) \quad (14)$$

This simplification cannot be performed for the expander as, unlike a volumetric pump, a closed-volume transformation takes place (expansion). The fluid inside the chambers is compressible, and the pressure and temperature change according to the volume variation and to the mechanical and thermal power exchanged. Therefore, to assess the

expander indicated power, the general expression (13) must be used.

The mechanical power required by the pump and that provided by the expander can be evaluated algebraically by adding and subtracting respectively the power loss by friction to the indicated power. Thus, for the pump and the expander, the mechanical power can be expressed as in (15) and (16), respectively:

$$P_{\text{mech,pmp}} = (P_{\text{ind,pmp}} + P_{\text{loss,pmp}}) \quad (15)$$

$$P_{\text{mech,exp}} = P_{\text{ind,exp}} - P_{\text{loss,exp}} \quad (16)$$

The power loss is generally given by the dry and viscous friction phenomena that occur between machine parts in relative motion. In particular, the dry friction phenomena represent nearly the total power loss due to friction for both the volumetric pump [40] and expander [25]. For the pump, the power loss due to friction is evaluated by dividing the mechanical power by the experimentally identified mechanical efficiency (17).

$$P_{\text{mech,pmp}} = \frac{P_{\text{ind,pmp}}}{\eta_{\text{pmp,mech}}} \quad (17)$$

Regarding the expander, the power loss is not evaluated through an equivalent approach, but according to the physical relation which expresses the dry friction generated by the rotor and stator surfaces (18), because the expander power loss is more sensitive to operating condition variations in comparison to the pump.

$$P_{\text{loss}} = fN_v F_N r_v \omega_{\text{exp}} \quad (18)$$

In (18), f represents the friction factor, N_v is the point of dry contact between the rotor and the stator (equal to the number of expander vanes), F_N is the normal force applied by the rotor on the stator at the contact point, and r_v is the distance between the force application point and rotor centre; (18) is generally applicable to all positive-displacement expanders and it can be specialised to a particular type defining a proper F_N which strictly depends on the expander technology and its geometric features. For instance, in the case of the SVRE employed in the experimental analysis, the normal force is given by the centrifugal force applied on the blades, pushing them against the stator inner surface. A further contribution, in this case, is also given by the fluid pressure enclosed under the blades when outstanding towards the stator.

Once the pump and expander mechanical power are evaluated, the ORC net power can be assessed (11); therefore, knowing the thermal power at the high thermal source $\dot{Q}_{\text{t,rec}}$, the overall ORC efficiency can be calculated as follows (19):

$$\eta_{\text{ORC}} = \frac{P_{\text{Net,ORC}}}{\dot{Q}_{\text{t,rec}}} \quad (19)$$

3.3. Model permeability validation

The model was validated by comparing the experimental intake pressure with the corresponding predicted values. The results are reported in Fig. 9(a), where it can be observed that the numerical prediction is close to the experimental data: a maximum deviation of 4.1% and a root mean square error (RMSE) of 1% are achieved. Moreover, the thermal power recovered at the evaporator was compared once the pressure and temperature at the expander intake were known. As can be observed in Fig. 9(b), the model yields a correct representation of this value, with an RMSE of 2.5%.

Another fundamental parameter is the volumetric efficiency of the expander. Typical initial values from the experimental experience are introduced as the volumetric efficiency and then updated by the model. The predictions are similar to the experimental data (Fig. 10), with a maximum deviation of 6.9% and an RMSE of 1.5%. The results of the validation can be considered satisfactory, owing to the good agreement between the experimental and theoretical data.

The validation results for the expander and pump power are shown in Fig. 11(a) and 11(b), respectively. It can be seen that an RMSE of 5% for the two machines was achieved. Moreover, the maximum deviation is comparable, being equal to 22.5% for the expander and 21% for the pump.

These results can be satisfactorily retained, considering the relative simplicity of the model. Indeed, a high rate of precision can be achieved with a more detailed model [25,40], which would require more computational resources.

4. Results and discussions

The analysis performed revealed that plant hydraulic permeability involves the following important aspects:

1. The permeability represents a constraint between the main operating parameters (i.e. mass flow rate and evaporating pressure). In other words, permeability defines the fixed operating paths along which these quantities may vary.
2. The permeability can be expressed as a function of the specific design and operating parameters according to the relationship expressed in Eqn. (8). Therefore, the operating path of an ORC-based power unit

can be varied by managing the three β parameters: speed ratio β_{ob} , volume ratio β_{vol} , and volumetric efficiencies $\beta_{\eta\text{v}}$.

3. The expander displacement volume and revolution speed are the only free parameters for properly varying plant permeability.

Considering these aspects, to deepen the understanding of and quantify how the design and operating ratios affect the permeability (overcoming the experimental constraints), the validated model of the recovery unit was used as a software platform. The analysis was performed with reference to the experimental data and varying each β parameter, keeping the others constant.

The definition of pump and expander displacement is one of the most important aspects of plant design, because it affects plant permeability. β_{vol} allows us to consider this effect and defines the optimal proportion between the pump displacement and expander displacement. β_{vol} is a design parameter that is defined *a priori* and cannot be changed during operation. The numerator is the pump swept volume V_{pmp} ; thus, it is proportional to the flow rate circulating inside the plant. On the contrary, the expander intake volume V_{exp} in the denominator indicates permeability. In previous sections, it was observed that for a certain mass flow rate range, the pump displacement volume must be considered together with the pump speed to fulfil the mass requirements. For a given V_{pmp} , the pump speed varies in a defined range, ensuring a linear increase in the intake pressure with mass flow rate (Fig. 5). Hence, the variation in V_{pmp} produces effects only on the pump speed range, which allows the mass flow rate requirements to be fulfilled without affecting the plant hydraulic impedance (Fig. 6). In contrast, the expander displaced volume affects the circuit hydraulic impedance and can be freely varied to achieve the desired permeability. Therefore, once the pump volume and revolution speed are optimised, β_{vol} varies, acting on the V_{exp} variation. Hence, for a given V_{pmp} , the higher the V_{exp} (the lower is β_{vol}), the higher is the permeability. In contrast, a reduction in permeability can be obtained by reducing V_{exp} . This feature can be seen in Fig. 12(a), where the intake pressure is reported as a function of mass flow rate, considering three different volume ratios (1.5, 2, and 3), the expander intake volume was set to 7, 5.4 (experimental case), and 4 cm³. The pump volume was maintained at the experimental value of 11.4 cm³. The other parameters assumed the experimental values ($\omega_{\text{exp}} = 1500$ rpm and $\beta_{\eta\text{v}} = 0.5$). The permeability is represented by the slope of the curve.

As Fig. 12(a) shows, the adoption of the maximum β_{vol} produces a lower expander permeability (0.11 kg/(sMPa)). Thus, following the theoretical expectation, this scenario ensures that the expander intake pressure varies between 14 and 35 bar, when the mass flow rate ranges from 0.1 kg/s to 0.4 kg/s. With a lower β_{vol} , the pressure range diminishes because of the increase in permeability. If $\beta_{\text{vol}} = 2$, the intake pressure ranges between 8 and 31 bar for mass flow rate varying from 0.08 and 0.4 kg/s.

The same phenomenon occurs for $\beta_{\text{vol}} = 1.5$; in this case, the pressure values further decrease. Fig. 12(b) shows the net power results: when $\beta_{\text{vol}} = 3$, the plant produces the highest power for mass flow rate up to 0.18 kg/s, whereas beyond this value, the maximum net power is achieved by adopting the minimum β_{vol} (1.5). This trend is a consequence of the increase in intake pressure with high β_{vol} (Fig. 12(a)), which for mass flow rate higher than 0.18 kg/s implies that the pump requires higher power with respect to the more permeable case ($\beta_{\text{vol}} = 1.5$). This is aspect is confirmed by the pump-to-expander power ratio (so-called 'backwork ratio') reported in Fig. 12(c). For a high mass flow rate (0.18–0.4) kg/s, a higher volume ratio implies that the impact of pump power on the expander ranges from 45% to 75%. The backwork ratio decreases for such mass flow rate values adopting low β_{vol} with pump power impact, which never exceeds 50%. As shown in Fig. 12(d), the increase in β_{vol} leads to an enhancement of the global efficiency for a lower mass flow rate (0.06–0.18) kg/s, with a maximum value equal to 3.5%. Nevertheless, as the mass flow rate increased, the maximum efficiency value could be assured by reducing $\beta_{\text{vol}} = 1.5$.

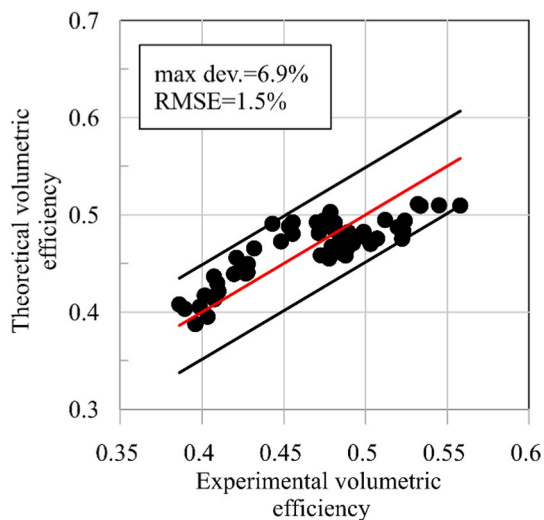


Fig. 10. Validation results: Comparison between experimental and predicted data of expander volumetric efficiency.

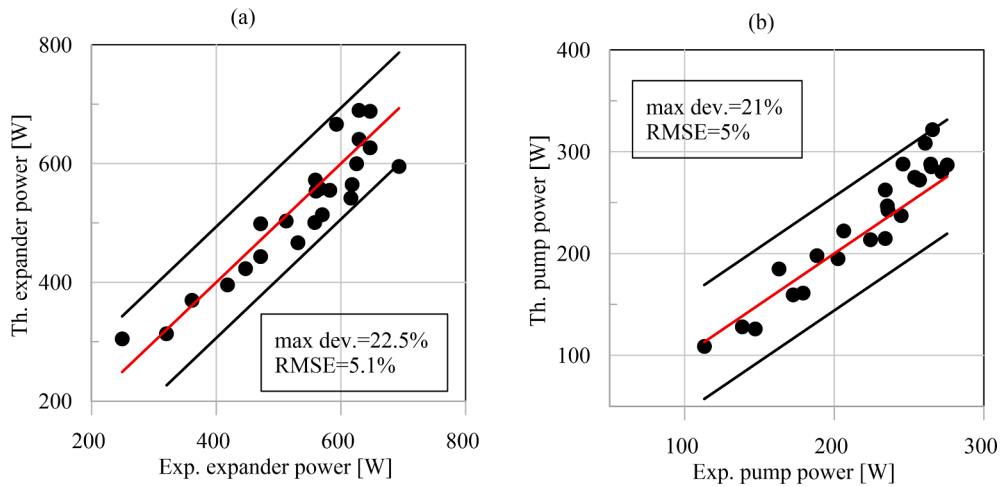


Fig. 11. Validation results: Comparison between experimental and predicted data for expander (a) and pump mechanical power (b).

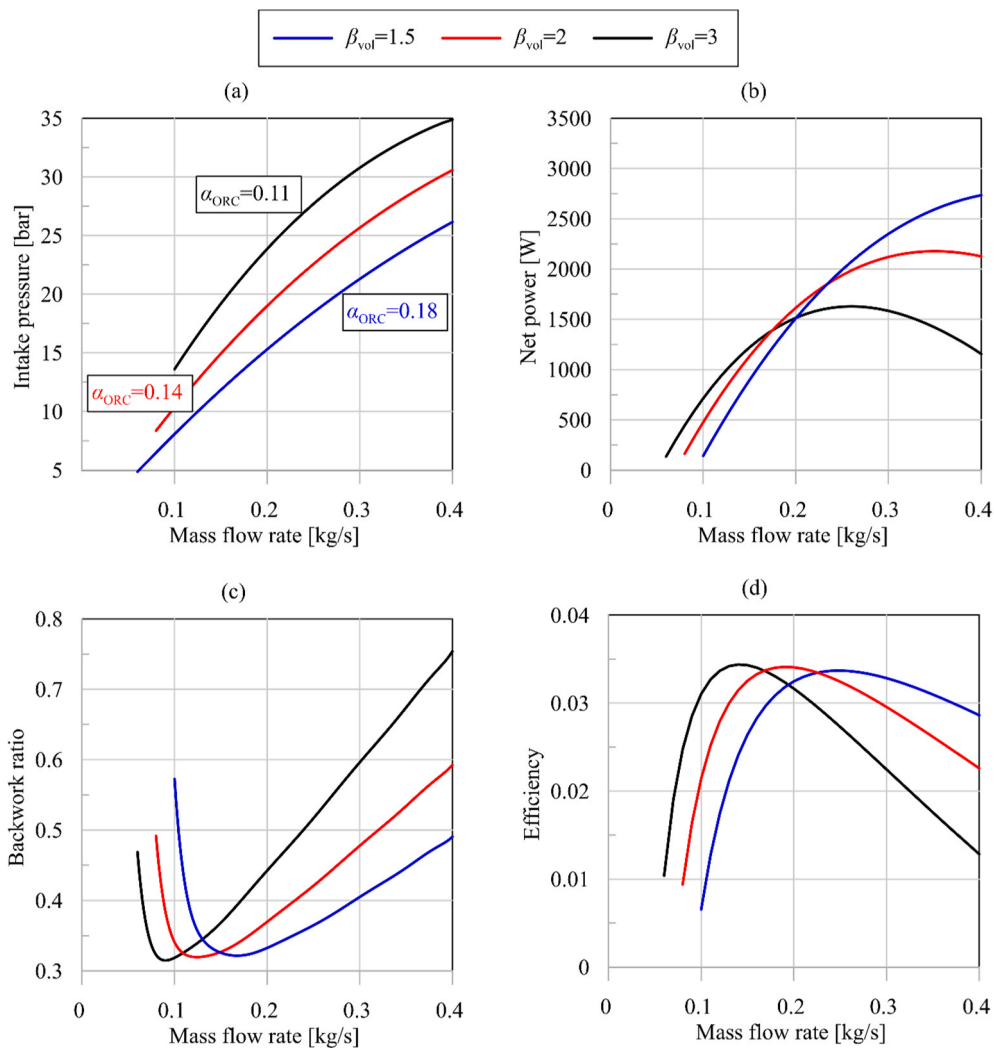


Fig. 12. Intake pressure (a), ORC net power (b), backwork ratio (c), and ORC efficiency (d) as functions of mass flow rate and volume ratio. The plant permeability is expressed in [kg/(sMPa)].

It is important to note that the effects of β_{vol} on plant performance must be observed relative to the considered mass flow rate range. This analysis indicates that the expander volume is too high or too low in comparison with the pump volume for a given mass flow rate interval.

Hence, keeping the pump displaced volume constant, if the mass flow rate is low, the choice of small expander volume (high β_{vol}) ensures that the best performance is achieved as the plant pressurisation is favoured. On the contrary, when the mass flow rate circulating grows, a large

expander volume (low β_{vol}) prevents the evaporating pressure from reaching extremely high values, leading to a high backwork ratio and safety concerns. In other words, once a mass flow rate range is defined, this parameter expresses the optimal proportion between the expander and pump volumes, allowing the achievement of proper plant pressurisation.

Considering the speed ratio β_ω , from (8), it can be noticed that the higher is β_ω , the lower is the permeability, and consequently, the higher is the evaporating pressure. Once the pump volume is defined, the pump speed varies within the same range to meet the mass flow rate requirements (500–1730 rpm). Therefore, the only free parameter to vary the permeability is the expander revolution speed, which ranges from 500 to 3000 rpm. Thus, keeping the mass flow rate circulating inside the plant constant (β_ω numerator) and setting the other design parameters equal to the experimental values ($\beta_{vol} = 2$ and $\beta_{\eta V} = 0.5$), if the expander rotates at a lower speed, the denominator diminishes, the permeability decreases, and consequently, the expander intake pressure increases (i.e. evaporating pressure). Thus, by properly varying the expander and pump speeds, the most appropriate β_ω can be set to achieve the desired plant permeability when the mass flow rate of the working fluid changes. In other words, by acting on β_ω , it is possible to implement a model-based control of the inlet expander pressure (maximum plant pressure) when the mass flow rate of the working fluid changes to allow

an increase in the mechanical power recovered as the enthalpy of the exhaust gases increases as well.

This result is shown in Fig. 13(a), where the expander intake pressure is reported as a function of the speed ratio and plant permeability. By setting a proper permeability (through the expander speed variation), the evaporating pressure can be continuously varied. For the mass flow rate range considered (0.1–0.4 kg/s), when the expander speed is fixed to 500 rpm, β_ω can range from 1 to 1.5, providing a pressure which varies between 30 and 35 bar. Indeed, in this case, the plant assumes the lowest permeability (0.05 kg/(s MPa)); moreover, a higher β_ω indicates that the pump speed is too high for the expander speed, such that the expander slowly elaborates the mass flow rate sent by the pump and its intake pressure grows.

In contrast, if the expander speed is higher (1500 or 3000 rpm), β_ω can diminish; thus, the expander is able to process the fluid provided by the pump faster, but with a consequent decrease in evaporating pressure. This is due to the plant permeability increase, which reaches values of 0.14 and 0.3 kg/(s MPa), respectively. Hence, the three cases reported in Fig. 13(a) represent different permeability situations, and the higher the permeability (which increases with expander speed), the narrower the β_ω range and the corresponding ORC top pressure values. In all the considered cases, the mass flow rate range was (0.1–0.4) kg/s.

The effect of β_ω was also evaluated in terms of the ORC net power

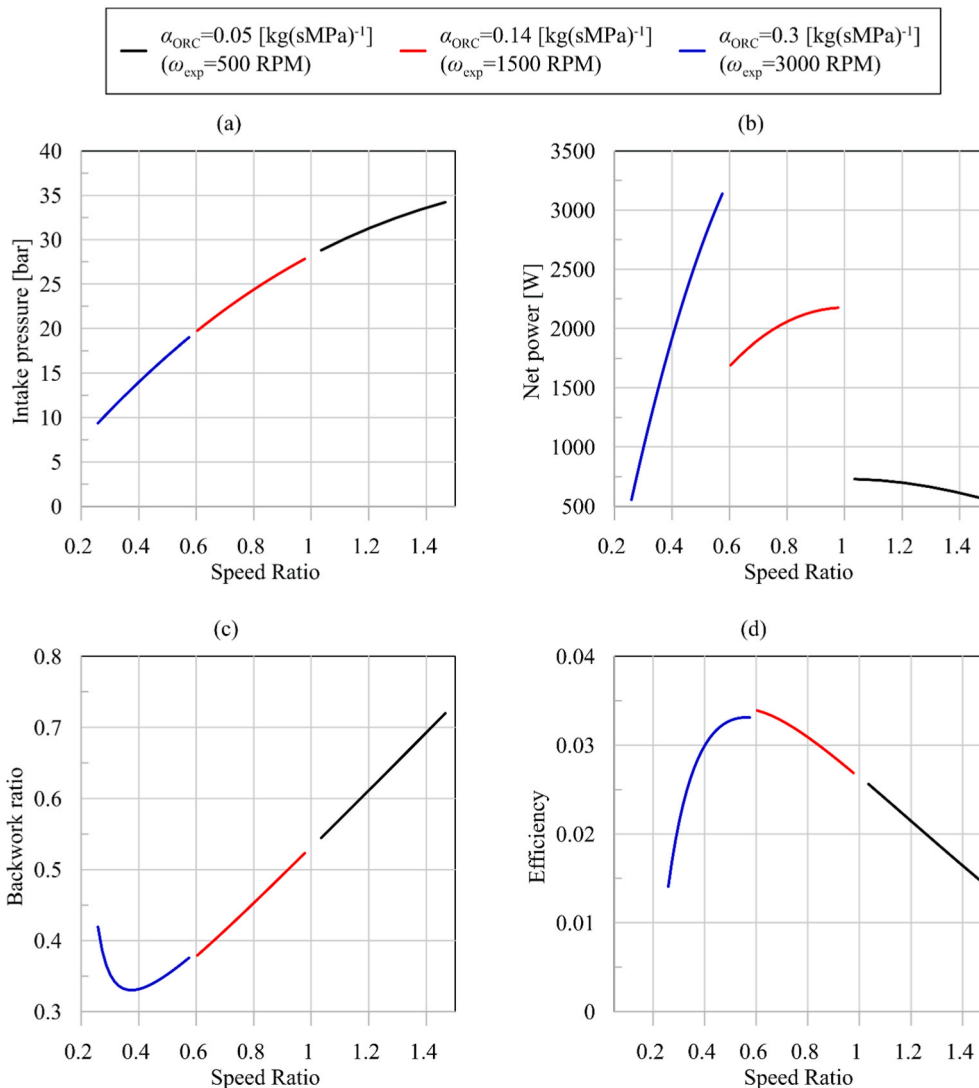


Fig. 13. Expander intake pressure (a), ORC net power (b), backwork ratio (c), and ORC efficiency (d) as functions of speed ratio. The plant permeability is expressed in [kg/(sMPa)].

(Fig. 13(b)). The maximum power (3.2 kW) is reached when β_{ω} is low (0.6), because in this case the expander performs more cycles per second and, thus, the indicated power increases Eqn. (13). A low β_{ω} corresponds to a high expander speed (3000 rpm); thus, the time required by the expander to complete one cycle diminishes. Nevertheless, the higher ORC net power at low β_{ω} is also due to the pump behaviour. Indeed, when the expander rotates at a high speed (low β_{ω}), the permeability increases, thus producing an expander intake pressure reduction. Therefore, keeping the minimum plant pressure constant (which depends on the low thermal source), the pressure rise of the pump is lower and the ORC net power grows consequently. This is also demonstrated by the backwork ratio, as shown in Fig. 13(c).

Therefore, a low β_{ω} produces the maximum ORC efficiency, as shown in Fig. 13(d). Here, it can be observed that for an expander speed of 3000 rpm and β_{ω} to 0.6, the ORC efficiency is equal to 3.5%. If the expander speed is 1500 rpm and the speed ratio varies between 0.6 and 1, the ORC efficiency is between 3.5% and 2.5%. Moreover, a higher β_{ω} leads to an ORC plant efficiency lower than 2.5%. Thus, it can be concluded that the best performance is achieved when the expander is able to quickly elaborate the mass flow rate provided by the pump (high expander speed). However, if the flow rate circulating inside the plant is low, it can be useful to reduce β_{ω} to decrease the permeability, which leads to a higher evaporating pressure (Fig. 13(a)).

The volumetric efficiency plays a fundamental role not only in the

definition of the pump and expander efficiency, but also in the permeability evaluation, and it can be considered in $\beta_{\eta v}$ which is the product between $\eta_{vol,pmp}$ and $\eta_{vol,exp}$. This parameter has a dual nature: it depends on both the design choice and operating conditions. The machine geometric features and constructive gap dimensions are the main design-related quantities. Nevertheless, this gap is often not only constructive (fixed), but also defined by force equilibrium (as in the case of sliding rotary vanes or scroll expanders). Therefore, operating conditions, such as expander speed and lubrication conditions, have an important role. The combined effects of the factor $\beta_{\eta v}$ on the ORC performance are shown in Fig. 14 in terms of evaporating pressure (a), ORC net power (b), backwork ratio (c), and ORC efficiency (d). In Fig. 14(a), it can be observed as with the increase in $\beta_{\eta v}$ (keeping $\omega_{exp} = 1500$ rpm and $\beta_{vol} = 2$) the plant permeability diminishes (0.12 kg/(s MPa)). This is due to the expander volumetric efficiency, which is lower if leakage occurs [25]. The net power output is affected by the efficiencies; the lower their value, the lower the ORC net power and efficiency (Fig. 14 (b) and (d)), because the leaked flow in the two machines is not useful, but it increases energy losses. If $\beta_{\eta v} = 0.3$, the ORC plant starts to produce power only for medium mass flow rate (0.11 kg/s), achieving a relatively modest maximum value (1000 W). In contrast, $\beta_{\eta v} = 0.6$ ensures the best plant performance both in terms of power values (maximum value equal to 2.5 kW) and operability range. However, such values require that the expander and pump have high volumetric

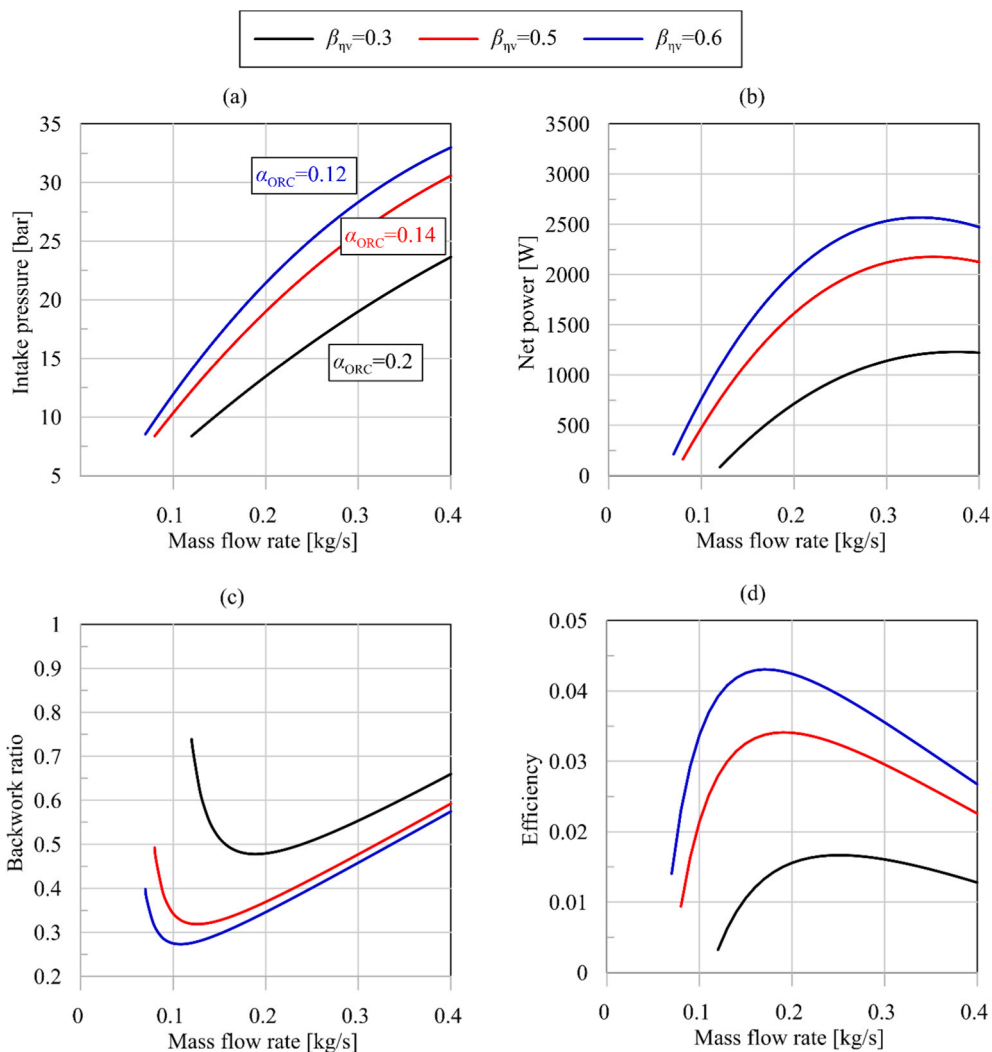


Fig. 14. Intake pressure (a), ORC Net Power (b), backwork ratio (c), and ORC efficiency (d) as functions of volumetric efficiency ratio and mass flow rate. The plant permeability is expressed in [kg/(sMPa)].

efficiency, which needs an improvement in the machine design and lubrication procedures. Finally, the improvement of $\beta_{\eta v}$ also favours better pressurisation of the power plant (lower permeability). This is demonstrated also by the backwork ratio, as shown in Fig. 14(c): in case of high $\beta_{\eta v}$, the impact of the pump on the expander power is always lower than in the other cases. All these aspects are mirrored in the global efficiency trend (Fig. 14(d)), which when $\beta_{\eta v} = 0.6$, reaches the maximum value of 4.4%.

5. Conclusions

In the present work, an experimental and theoretical characterisation was conducted to analyse the impact of the hydraulic permeability of an ORC-based power unit on the recovery performance. The permeability represents the attitude of the plant to be crossed by the working fluid, and is defined by the pump and expander matching. By expressing the mass conservation as the balance between the mass flow rate provided by the pump and that elaborated by the expander, it is possible to define the permeability relation as a function of nonlinear parameters. Nevertheless, the results of the experimental campaign performed on the ORC-based power unit, fed by the exhaust gases of a 3 L diesel engine, show that even if these non-linearities are neglected, the phenomena can be accurately represented. Based on this knowledge, a theoretical model of the ORC-based power unit was developed, and it was used to deepen the permeability concept after extensive experimental validation. Based on the model and its validation, it was observed that one of the main effects of plant permeability is the definition of the operating paths of the recovery unit which correspond to a specific correlation between operating quantities. This aspect is important, as it implies that the permeability definitively introduces a constraint between the operating quantities, limiting the domain in which the operating conditions (maximum pressure, mass flow rate, expander, and pump speeds) can be varied. The theoretical comprehensive model of the ORC plant also allows a discussion of how permeability affects plant performance following a novel theoretical approach. This consists of the definition of the permeability relationship as a function of the following dimensionless parameters:

- β_{ω} , which expresses the pump-to-expander revolution speed ratio;
- β_{vol} , which expresses the pump discharge to expander intake volume ratio;
- $\beta_{\eta v}$, which indicates the product of the pump and expander volumetric efficiencies.

The obtained results are summarized as follows:

- By increasing β_{ω} , different plant permeabilities can be obtained, depending mainly on the expander revolution speed. When β_{ω} is 0.6, the best performance is achieved in terms of the ORC efficiency (3.5%) and net power (3 kW).
- β_{vol} indicates a dimensionless relationship between the pump displacement and expander intake volume. Thus, it defines the best machine geometric proportion, which ensures suitable pressurisation of the plant.
- The analysis of $\beta_{\eta v}$ highlights that the volumetric efficiency is certainly the performance parameter of the pump and expander which most strongly affects the ORC plant performance. The higher this value, the higher is the ORC performance and operability range. When $\beta_{\eta v}$ is 0.6, ORC efficiency of 4.4% is achieved.

Therefore, the developed model-based approach can be adopted to perform an appropriate selection of the main design (β_{vol} and $\beta_{\eta v}$) and to set the operating parameters (β_{ω}) which maximise the recovery and efficiency. Indeed, this novel approach allows us to carry out an integrated design of volumetric machines and guarantee that the plant operates to the greatest extent possible under optimal conditions. This design

optimisation cannot be performed by separately treating the pump and expander, as the permeability links their interaction.

CRedit authorship contribution statement

Fabio Fatigati: Conceptualization, Investigation, Methodology, Software, Validation, Data curation, Writing - original draft, Writing - review & editing. **Davide Di Battista:** Conceptualization, Investigation, Methodology, Validation, Data curation, Writing - original draft, Writing - review & editing. **Roberto Cipollone:** Visualization, Investigation, Conceptualization, Methodology, Supervision, Writing - review & editing.

Declaration of Competing Interest

The authors declare that they have no known competing financial interests or personal relationships that could have appeared to influence the work reported in this paper.

Acknowledgements

The study was performed within the framework of the EU project "LONGRUN - Development of efficient and environmental friendly LONG distance powertrain for heavy duty trucks and coaches".

The study also benefited from the support of the National Operating Program (PON) for Attraction and International Mobility (AIM) - AIM1829299, a project of the Italian Ministry of University (MIUR) to favour international research collaboration.

References

- [1] IEA, Transport sector CO₂ emissions by mode in the Sustainable Development Scenario, 2000-2030, IEA, Paris. <https://www.iea.org/data-and-statistics/charts/transport-sector-co2-emissions-by-mode-in-the-sustainable-development-scenario-2000-2030>.
- [2] D.B. Gohil, A. Pesyridis, J.R. Serrano, Overview of Clean Automotive Thermal Propulsion Options for India to 2030, Appl. Sci. 10 (10) (2020) 3604, <https://doi.org/10.3390/app10103604>.
- [3] J. Song, X. Li, K. Wang, C.N. Markides, Parametric optimisation of a combined supercritical CO₂ (S-CO₂) cycle and organic Rankine cycle (ORC) system for internal combustion engine (ICE) waste-heat recovery, Energy Conversion Manage. 218 (2020), <https://doi.org/10.1016/j.enconman.2020.112999>. ISSN 0196-8904.
- [4] R. Cipollone, D. Di Battista, A. Perosino, F. Bettoja, Waste Heat Recovery by an Organic Rankine Cycle for Heavy Duty Vehicles - SAE Technical paper, 2016-01-023.
- [5] D. Di Battista, F. Fatigati, R. Carapellucci, R. Cipollone, An improvement to waste heat recovery in internal combustion engines via combined technologies, Energy Conversion Manage. 232 (2021), <https://doi.org/10.1016/j.enconman.2021.113880>.
- [6] D. Di Battista, M. Mauriello, R. Cipollone, Effects of an ORC based heat recovery system on the performances of a diesel engine, SAE Technical Paper 2015-01-1608 (2015), <https://doi.org/10.4271/2015-01-1608>.
- [7] X. Wu, J. Chen, L. Xie, Optimal design of organic Rankine cycles for exhaust heat recovery from light-duty vehicles in view of various exhaust gas conditions and negative aspects of mobile vehicles, Appl. Thermal Eng. 179 (2020), <https://doi.org/10.1016/j.applthermaleng.2020.115645>.
- [8] K. Rosset, V. Mounier, E. Guenat, J. Schifffmann, Multi-objective optimization of turbo-ORC systems for waste heat recovery on passenger car engines, Energy 159 (2018) 751-765, <https://doi.org/10.1016/j.energy.2018.06.193>. ISSN 0360-5442.
- [9] D. Di Battista, M. Di Bartolomeo, C. Villante, R. Cipollone, A Model Approach to the Sizing of an ORC Unit for WHR in Transportation Sector, SAE Int. J. Commer. Veh. 10 (2) (2017), <https://doi.org/10.4271/2017-24-0159>.
- [10] D. Di Battista, M. Di Bartolomeo, C. Villante, R. Cipollone, On the limiting factors of the waste heat recovery via ORC-based power units for on-the-road transportation sector, Energy Conversion Manage. 155 (2018) 68-77, <https://doi.org/10.1016/j.enconman.2017.10.091>. ISSN 0196-8904.
- [11] M.A. Chatzopoulou, M. Simpson, P. Sapin, C.N. Markides, Off-design optimisation of organic Rankine cycle (ORC) engines with piston expanders for medium-scale combined heat and power applications, Appl. Energy 238 (2019) 1211-1236, <https://doi.org/10.1016/j.apenergy.2018.12.086>. ISSN 0360-2619.
- [12] S. Seyedkavoosi, S. Javan, K. Kota, Exergy-based optimization of an organic Rankine cycle (ORC) for waste heat recovery from an internal combustion engine (ICE), Appl. Thermal Eng. 126 (2017) 447-457, <https://doi.org/10.1016/j.applthermaleng.2017.07.124>. ISSN 1359-4311.
- [13] Y. Fang, F. Yang, H. Zhang, Comparative analysis and multi-objective optimization of organic Rankine cycle (ORC) using pure working fluids and their zeotropic

- mixtures for diesel engine waste heat recovery, *Appl. Thermal Eng.* 157 (2019), <https://doi.org/10.1016/j.applthermaleng.2019.04.114>. ISSN 1359-4311.
- [14] H. Tian, G. Shu, H. Wei, X. Liang, L. Liu, Fluids and parameters optimization for the organic Rankine cycles (ORCs) used in exhaust heat recovery of Internal Combustion Engine (ICE), *Energy* 47 (1) (2012) 125–136, <https://doi.org/10.1016/j.energy.2012.09.021>. ISSN 0360-5442.
- [15] R. Scaccabarozzi, M. Tavano, C. Mario Invernizzi, E. Martelli, Comparison of working fluids and cycle optimization for heat recovery ORCs from large internal combustion engines, *Energy* 158 (2018) 396–416, <https://doi.org/10.1016/j.energy.2018.06.017>. ISSN 0360-5442.
- [16] E.H. Wang, H.G. Zhang, B.Y. Fan, M.G. Ouyang, Y. Zhao, Q.H. Mu, Study of working fluid selection of organic Rankine cycle (ORC) for engine waste heat recovery, *Energy* 36 (5) (2011) 3406–3418, <https://doi.org/10.1016/j.energy.2011.03.041>. ISSN 0360-5442.
- [17] R. Dickes, O. Dumont, V. Lemort, Experimental assessment of the fluid charge distribution in an organic Rankine cycle (ORC) power system, *Appl. Thermal Eng.* 179 (2020), <https://doi.org/10.1016/j.applthermaleng.2020.115689>. ISSN 1359-4311.
- [18] R. Dickes, O. Dumont, L. Guillaume, S. Quoilin, V. Lemort, Charge-sensitive modelling of organic Rankine cycle power systems for off-design performance simulation, *Appl. Energy* 212 (2018) 1262–1281, <https://doi.org/10.1016/j.apenergy.2018.01.004>. ISSN 0306-2619.
- [19] M. Marchionni, G. Bianchi, A. Karvountzis-Kontakiotis, A. Pesyridis, S.A. Tassou, An appraisal of proportional integral control strategies for small scale waste heat to power conversion units based on Organic Rankine Cycles, *Energy* 163 (2018) 1062–1076, <https://doi.org/10.1016/j.energy.2018.08.156>. ISSN 0360-5442.
- [20] L. Guillaume, V. Lemort, Comparison of different ORC typologies for heavy-duty trucks by means of a thermo-economic optimization, *Energy* 182 (2019) 706–728, <https://doi.org/10.1016/j.energy.2019.05.195>. ISSN 0360-5442.
- [21] F. Pantano, R. Capata, Expander selection for an on board ORC energy recovery system, *Energy* 141 (2017) 1084–1096, <https://doi.org/10.1016/j.energy.2017.09.142>. ISSN 0360-5442.
- [22] R. Cipollone, G. Bianchi, M. Di Bartolomeo, D. Di Battista, F. Fatigati, Low grade thermal recovery based on trilateral flash cycles using recent pure fluids and mixtures, *Energy Procedia* 123 (2017) 289–296.
- [23] G. Qiu, H. Liu, S. Riffat, Expanders for micro-CHP systems with organic Rankine cycle, *Appl. Thermal Eng.* 31 (16) (2011) 3301–3307, <https://doi.org/10.1016/j.applthermaleng.2011.06.008>. ISSN 1359-4311.
- [24] V. Vodicka, V. Novotny, J. Mascuch, M. Kolovratnik, Impact of major leakages on characteristics of a rotary vane expander for ORC, *Energy Procedia* 129 (2017) 387–394, <https://doi.org/10.1016/j.egypro.2017.09.249>. ISSN 1876-6102.
- [25] F. Fatigati, M. Di Bartolomeo, R. Cipollone, On the effects of leakages in Sliding Rotary Vane Expanders, *Energy* 192 (2020), <https://doi.org/10.1016/j.energy.2019.116721>. ISSN 0360-5442.
- [26] N. Casari, E. Fadiga, M. Pinelli, S. Randi, A. Suman, D. Ziviani, Investigation of flow characteristics in a single screw expander: A numerical approach, *Energy* 213 (2020), <https://doi.org/10.1016/j.energy.2020.118730>. ISSN 0360-5442.
- [27] S. Rane, A. Kovačević, N. Stojić, I. Smith, Analysis of real gas equation of state for CFD modelling of twin-screw expanders with R245fa, R290, R1336mzz(Z) and R1233zd(E), *International Journal of Refrigeration*, Volume 121, 2021, Pages 313–326, ISSN 0140-7007, Doi: 10.1016/j.ijrefrig.2020.10.022.
- [28] Y. Han, Y. Zhang, T. Zuo, R. Chen, Y. Xu, Experimental study and energy loss analysis of an R245fa organic Rankine cycle prototype system with a radial piston expander, *Appl. Thermal Eng.* 169 (2020), <https://doi.org/10.1016/j.applthermaleng.2020.114939>. ISSN 1359-4311.
- [29] J. Gao, C. Ma, G. Tian, S. Xing, P. Jenner, Numerical investigations of an opposed rotary piston expander for the purpose of the applications to a small-scale Rankine cycle, *Appl. Thermal Eng.* 82 (2021), <https://doi.org/10.1016/j.applthermaleng.2020.116157>. ISSN 1359-4311.
- [30] G. Rossi Fanti, D. Araújo Romão, R. Barbosa de Almeida, P.E. Batista de Mello, Influence of flank clearance on the performance of a scroll expander prototype, *Energy* 193 (2020), <https://doi.org/10.1016/j.energy.2019.116823>. ISSN 0360-5442.
- [31] J. Oh, H. Jeong, J. Kim, H. Lee, Numerical and experimental investigation on thermal-hydraulic characteristics of a scroll expander for organic Rankine cycle, *Appl. Energy* 278 (2020), <https://doi.org/10.1016/j.apenergy.2020.115672>. ISSN 0306-2619.
- [32] B. Yang, X. Peng, Z. He, B. Guo, Z. Xing, Experimental investigation on the internal working process of a CO2 rotary vane expander, *Appl. Thermal Eng.* 29 (11-12) (2009) 2289–2296, <https://doi.org/10.1016/j.applthermaleng.2008.11.023>. ISSN 1359-4311.
- [33] V. Vodicka, V. Novotny, Z. Zeleny, J. Mascuch, M. Kolovratnik, Theoretical and experimental investigations on the radial and axial leakages within a rotary vane expander, *Energy* 189 (2019), <https://doi.org/10.1016/j.energy.2019.116097>. ISSN 0360-5442.
- [34] P. Kolański, Experimental and modelling studies on the possible application of heat storage devices for powering the ORC (organic rankine cycle) systems, *Thermal Sci. Eng. Prog.* 19 (2020), <https://doi.org/10.1016/j.tsep.2020.100586>. ISSN 2451-9049.
- [35] F. Fatigati, M. Di Bartolomeo, D. Di Battista, R. Cipollone, Experimental and Numerical Characterization of the Sliding Rotary Vane Expander Intake Pressure in Order to Develop a Novel Control-Diagnostic Procedure, *Energies* 2019 (1970) 12, <https://doi.org/10.3390/en12101970>.
- [36] F. Fatigati, M. Di Bartolomeo, D. Di Battista, R. Cipollone, Experimental characterization of a hermetic scroll expander operating in an ORC-based power unit bottoming an internal combustion engine, *AIP Conf. Proc.* 2191 (2019), 020069, <https://doi.org/10.1063/1.5138802>.
- [37] F. Fatigati, M. Di Bartolomeo, D. Di Battista, R. Cipollone, A dual-intake-port technology as a design option for a Sliding Vane Rotary Expander of small-scale ORC-based power units, *Energy Conversion Manage.* 209 (2020), <https://doi.org/10.1016/j.enconman.2020.112646>. ISSN 0196-8904.
- [38] F. Fatigati, M. Di Bartolomeo, R. Cipollone, Dual intake rotary vane expander technology: Experimental and theoretical assessment, *Energy Conversion Manage.* 186 (2019) 156–167, <https://doi.org/10.1016/j.enconman.2019.02.026>. ISSN 0196-8904.
- [39] L. Pan, H. Wang, W. Shi, Regulation law of turbine and generator in organic Rankine cycle power generation experimental system, *Trans. Tianjin Univ.* 20 (2014) 237–242, <https://doi.org/10.1007/s12209-014-2220-z>.
- [40] G. Bianchi, F. Fatigati, S. Murgia, R. Cipollone, Design and analysis of a sliding vane pump for waste heat to power conversion systems using organic fluids, *Appl. Thermal Eng.* 124 (2017) 1038–1048, <https://doi.org/10.1016/j.applthermaleng.2017.06.083>. ISSN 1359-4311.


Io sottoscritto Fabio Fatigati, co-autore dell'articolo scientifico: "Permeability effects assessment on recovery performances of small-scale ORC plant" pubblicato sulla rivista internazionale Applied Thermal Engineering, (<https://doi.org/10.1016/j.applthermaleng.2021.117331>), dichiaro che i contributi degli autori nello sviluppo del presente articolo sono i seguenti:

- **Fabio Fatigati:** Conceptualization, Investigation, Methodology, Software, Validation, Data curation, Writing - original draft, Writing – review & editing;
- **Davide Di Battista:** Conceptualization, Investigation, Methodology, Validation, Data curation, Writing - original draft, Writing - review & editing;
- **Roberto Cipollone:** Visualization, Investigation, Conceptualization, Methodology, Supervision, Writing - review & editing.

L'indicazione sui contributi degli autori è riportata nel *CRedit* *authorship contribution statement* a pagina 16 del medesimo articolo.

In fede, L'Aquila 24/09/2021

Fabio Fatigati

A handwritten signature in black ink, appearing to read 'Fabio Fatigati', is written over a horizontal line.